

# Journal of Visualized Experiments

## Three-dimensional In Vitro Biomimetic Model of Neuroblastoma Using Collagen-based Scaffolds --Manuscript Draft--

Article Type:	Invited Methods Collection - JoVE Produced Video
Manuscript Number:	JoVE62627R2
Full Title:	Three-dimensional In Vitro Biomimetic Model of Neuroblastoma Using Collagen-based Scaffolds
Corresponding Author:	Olga Piskareva Royal College of Surgeons in Ireland Dublin, Dublin IRELAND
Corresponding Author's Institution:	Royal College of Surgeons in Ireland
Corresponding Author E-Mail:	olgapiskareva@rcsi.ie
Order of Authors:	Ciara Gallagher Catherine Murphy Fergal O'Brien Olga Piskareva
Additional Information:	
Question	Response
Please specify the section of the submitted manuscript.	Cancer Research
Please indicate whether this article will be Standard Access or Open Access.	Open Access (\$3900)
Please indicate the <b>city, state/province, and country</b> where this article will be <b>filmed</b> . Please do not use abbreviations.	Dublin, Ireland
Please confirm that you have read and agree to the terms and conditions of the author license agreement that applies below:	I agree to the <a href="#">Author License Agreement</a>
Please provide any comments to the journal here.	

**TITLE:**

Three-dimensional *In Vitro* Biomimetic Model of Neuroblastoma Using Collagen-based Scaffolds

**AUTHORS AND AFFILIATIONS:**

Ciara Gallagher<sup>\*,1,2,3</sup>, Catherine Murphy<sup>\*,1,2,3</sup>, Fergal O'Brien<sup>3,4,5</sup>, Olga Piskareva<sup>1,2,3,5,6</sup>

<sup>1</sup>Cancer Bioengineering Group, Department of Anatomy and Regenerative Medicine, RCSI University of Medicine and Health Sciences, Dublin, Ireland

<sup>2</sup>School of Pharmacy and Biomolecular Sciences, RCSI University of Medicine and Health Sciences, Dublin, Ireland

<sup>3</sup>Tissue Engineering Research Group, Department of Anatomy and Regenerative Medicine, RCSI University of Medicine and Health Sciences, Dublin, Ireland

<sup>4</sup>Trinity Centre for Bioengineering, Trinity College Dublin, Dublin, Ireland

<sup>5</sup>Advanced Materials and Bioengineering Research Centre (AMBER), RCSI and TCD, Dublin, Ireland

<sup>6</sup>National Children's Research Centre, OLCHC, Dublin, Ireland

\*Authors contributed equally

**Email addresses of co-authors:**

Ciara Gallagher ([ciaragallagher@rcsi.com](mailto:ciaragallagher@rcsi.com))

Catherine Murphy ([catherinemurphy@rcsi.com](mailto:catherinemurphy@rcsi.com))

Fergal O'Brien ([fjobrien@rcsi.com](mailto:fjobrien@rcsi.com))

**Corresponding author:**

Olga Piskareva ([olgapiskareva@rcsi.com](mailto:olgapiskareva@rcsi.com))

**SUMMARY:**

This paper lists the steps required to seed neuroblastoma cell lines on previously described three-dimensional collagen-based scaffolds, maintain cell growth for a predetermined timeframe, and retrieve scaffolds for several cell growth and cell behavior analyses and downstream applications, adaptable to satisfy a range of experimental aims.

**ABSTRACT:**

Neuroblastoma is the most common extracranial solid tumor in children, accounting for 15% of overall pediatric cancer deaths. The native tumor tissue is a complex three-dimensional (3D) microenvironment involving layers of cancerous and non-cancerous cells surrounded by an extracellular matrix (ECM). The ECM provides physical and biological support and contributes to disease progression, patient prognosis, and therapeutic response.

This paper describes a protocol for assembling a 3D scaffold-based system to mimic the neuroblastoma microenvironment using neuroblastoma cell lines and collagen-based scaffolds. The scaffolds are supplemented with either nanohydroxyapatite (nHA) or glycosaminoglycans (GAGs), naturally found at high concentrations in the bone and bone marrow, the most common metastatic sites of neuroblastoma. The 3D porous structure of these scaffolds allows

neuroblastoma cell attachment, proliferation and migration, and the formation of cell clusters. In this 3D matrix, the cell response to therapeutics is more reflective of the *in vivo* situation.

The scaffold-based culture system can maintain higher cell densities than conventional two-dimensional (2D) cell culture. Therefore, optimization protocols for initial seeding cell numbers are dependent on the desired experimental timeframes. The model is monitored by assessing cell growth via DNA quantification, cell viability via metabolic assays, and cell distribution within the scaffolds via histological staining.

This model's applications include the assessment of gene and protein expression profiles as well as cytotoxicity testing using conventional drugs and miRNAs. The 3D culture system allows for the precise manipulation of cell and ECM components, creating an environment more physiologically similar to native tumor tissue. Therefore, this 3D *in vitro* model will advance the understanding of the disease pathogenesis and improve the correlation between results obtained *in vitro*, *in vivo* in animal models, and human subjects.

## INTRODUCTION:

Neuroblastoma is a pediatric cancer of the sympathetic nervous system arising during embryonic development or early post-natal life due to the transformation of neural crest cells<sup>1</sup>. It is the most common solid extracranial tumor in children, representing 8% of the malignancies diagnosed in patients under 15 years and is responsible for 15% of all childhood cancer deaths. The disease displays highly heterogeneous clinical behaviors due to specific chromosomal, genetic and epigenetic alterations, and histopathology features.

These alterations contribute to the aggressiveness of neuroblastoma and poor outcomes in pediatric patients. Hence, current therapies prove ineffective in the long term for almost 80% of patients with the clinically aggressive disease<sup>2</sup>, highlighting the fact that treatment for this group of patients remains challenging. This is likely due to the mechanisms of neuroblastoma heterogeneity and metastases still not being fully understood. However, the tumor microenvironment (TME) is now widely believed to play a role in the progression of many cancers; yet it remains understudied in neuroblastoma<sup>3,4</sup>.

The native TME is a complex 3D microenvironment involving cancerous and non-cancerous cells surrounded by an ECM. The ECM refers to the acellular component of a tissue that provides structural and biochemical support to its cellular residents and contributes to disease progression, patient prognosis, and therapeutic response<sup>5</sup>. This promotion of disease progression is due to "dynamic reciprocity" or ongoing bidirectional communication between cells and the ECM<sup>6-8</sup>. As cancer progresses, stromal collagen is reorganized often in linear patterns perpendicular to the stroma-cancer interface, which cancer cells use as a migratory route to metastasis<sup>9-11</sup>.

The main components of this native functional biological scaffold include a fibrous network of collagens type I and II and other proteins, including elastin, glycoproteins such as laminin, as well as a range of proteoglycans and other soluble components<sup>12,13</sup>. These proteins of the native ECM

have now become attractive natural biomolecules for developing 3D *in vitro* models<sup>3</sup>. The application of 3D scaffolds for *in vitro* cell culture is increasing in popularity owing to its greater physiological representation of the TME compared to traditional 2D monolayer culture. The manufactured 3D scaffolds assist cell attachment, proliferation, migration, metabolism, and response to stimuli seen in *in vivo* biological systems.

The principal component of these 3D scaffolds is collagen, which is a key player in many normal biological processes including tissue repair, angiogenesis, tissue morphogenesis, cell adhesion, and migration<sup>11</sup>. Collagen-based 3D matrices have shown their robust functionality to model ECM, serving as an *in vitro* biomimetic microenvironment while enabling cell-ECM interactions as well as cell migration and invasion. These 3D matrices also provide a more accurate analysis of cell response to chemotherapeutic drugs than traditional 2D or “flat” culture in many cancer models<sup>14–16</sup>, including neuroblastoma<sup>17,18</sup>. Genetic analysis of 3D cell cultures has reported a higher correlation with the human tissue profile even when compared to animal models<sup>19</sup>. Overall, the cornerstone of these 3D scaffolds is to provide cells a suitable *in vitro* environment, which recapitulates the native tissue architecture and facilitates bidirectional molecular crosstalk<sup>8</sup>.

To increase the complexity of collagen-based models, other common ECM components are incorporated in the tissue engineering process, thus creating more physiologically relevant models to reflect niche TMEs of different tissues. For example, GAGs, negatively charged polysaccharides present in all mammalian tissues<sup>20</sup>, facilitate cell attachment, migration, proliferation, and differentiation. Chondroitin sulfate is a specific type of GAG found in the bone and cartilage, which has been previously used in tissue engineering applications for bone repair<sup>21–25</sup>. Nano-hydroxyapatite (nHA) is the main inorganic constituent of the mineral composition of human bone tissues, constituting up to 65% of bone by weight<sup>26</sup> and is therefore widely used for bone replacement and regeneration<sup>27</sup>. Thus, GAGs and nHA are attractive composites for reconstructing the primary neuroblastoma ECM and modeling the most common metastatic sites of neuroblastoma, bone marrow (70.5%), and bone (55.7%)<sup>28</sup>.

Scaffolds incorporating these ECM components were originally developed for bone tissue engineering applications with extensive analysis of their biocompatibility, toxicity, and osteoconductive and osteoinductive features<sup>29,30</sup>. They are porous, collagen-based matrices produced using freeze-drying techniques to control their physical and biological properties. The collagen scaffolds supplemented with either nHA (Coll-I-nHA) or chondroitin-6-sulfate (Coll-I-GAG) demonstrated success in mimicking the primary TME in breast cancer<sup>31</sup> and metastasis to bone in prostate cancer<sup>15</sup> as well as neuroblastoma<sup>17</sup>. The freeze-drying technique used to manufacture these composite scaffolds yields reproducible homogeneity in pore size and porosity within the scaffolds<sup>22–24</sup>. Briefly, a collagen slurry (0.5 wt%) is fabricated by blending fibrillar collagen with 0.05 M acetic acid. For Coll-I-GAG, 0.05 wt% of chondroitin-6-sulfate isolated from shark cartilage is added to the collagen slurry while blending.

For the composite Coll-I-nHA scaffolds, nano-sized hydroxyapatite particles are synthesized as previously described<sup>27</sup> and added to the collagen slurry at a 2:1 ratio to the weight of the collagen



during the blending process. All scaffolds are physically crosslinked and sterilized using a dehydrothermal treatment at 105 °C for 24 h<sup>25</sup>. Cylindrical scaffolds (6 mm diameter, 4 mm height) are obtained using a biopsy punch and can be chemically crosslinked with 3 mM N-(3-dimethylaminopropyl)-N'-ethylcarbodiimide hydrochloride and 5.5 mM N-hydroxysuccinimide (EDAC/NHS) in distilled water (dH<sub>2</sub>O) to improve the mechanical properties of the constructs<sup>30</sup>. This well-optimized manufacturing process of two collagen scaffolds creates scaffolds with reproducible mechanical properties, including pore size, porosity, and stiffness (kPa). Both Coll-I-GAG and Coll-I-nHA scaffolds have varying physical properties, creating different environmental conditions. The properties of each scaffold are displayed in **Table 1**.

[PLACE TABLE 1 HERE]

This paper describes a protocol of assembling a 3D scaffold-based system to better mimic the neuroblastoma microenvironment using neuroblastoma cell lines and previously described collagen-based scaffolds supplemented with either nHA (Coll-I-nHA) or chondroitin-6-sulphate (Coll-I-GAG). The protocol includes downstream methods to analyze the growth mechanisms of the neuroblastoma cells in a more physiologically relevant environment using previously optimized inexpensive methods adapted from 2D monolayer culture **Figure 1**.

[PLACE FIGURE 1 HERE]

## **PROTOCOL:**

### **1. Experimental design**

NOTE: The number of scaffolds and cells needed for each experiment will be dependent on the scale of the experiment and can be calculated using the tools in this section on experimental design.

#### **1.1. Number of scaffolds required**

1.1.1. Determine the overall experimental timeline and assessment intervals for changes in cell biology (e.g., cell growth and metabolism).

NOTE: For example, the experimental timeframe is 14 days, with an assessment of cell growth every 7 days. Thus, the experimental time points are Days 1, 7, 14 giving a total of 3 time points.

1.1.2. Next, decide the number of experimental applications to be applied at each time point. Try to complete the same analyses at every time point to monitor the changes.

NOTE: Typical analyses of cell growth on scaffolds include cell viability assays, DNA quantification, histological staining and imaging, and gene expression analysis. These will be further discussed in section 5.

1.1.3. Decide when to use the same scaffold for multiple downstream applications, e.g., after cell viability assessment using an appropriate assay, re-use the scaffold for DNA/RNA isolation (discussed in 5.1.11).

1.1.4. Keep a minimum of 3 biological replicates for each application, e.g., 3 scaffolds for cell viability and DNA quantification, 3 for histology, and 3 for gene expression analysis. As this equals 9 scaffolds per time point, plan to use 27 scaffolds for 3 time points.

1.1.5. Finally, multiply this number by the number of experimental parameters or conditions (e.g., assessing multiple cell lines, initial seeding densities, scaffold compositions).

NOTE: In this protocol, 4 different initial seeding densities were being assessed for one cell line, resulting in 108 (27 scaffolds x 4 conditions) scaffolds required. To account for human error and give extra coverage, add ~10% to this number, e.g., if 108 scaffolds are required, prepare 120 scaffolds.

## 1.2. Number of cells required

NOTE: A 20  $\mu$ L volume of cell suspension is recommended for seeding cells onto a cylindrical scaffold (diameter 6 mm, height 4 mm) on Day 0. The number of cells per this 20  $\mu$ L of cell suspension is adjusted according to the experimental design, calculated in section 1.1. A common initial seeding density is  $2 \times 10^5$  cells per 20  $\mu$ L, used as an example for the below protocol.

1.2.1. To calculate the total amount of cells required for the experiment, multiply the initial  $2 \times 10^5$  cells per 20  $\mu$ L by the number of scaffolds required.

NOTE: For example, 30 scaffolds multiplied by 20  $\mu$ L gives a total volume of 600  $\mu$ L. If each scaffold requires  $2 \times 10^5$  cells, 600  $\mu$ L of suspension contains a total of  $6 \times 10^6$  cells ( $2 \times 10^5 \times 30$ ), giving a final requirement of  $6 \times 10^6$  cells in 600  $\mu$ L. The number of the experimental parameters will dictate the total number of cells required. This protocol, therefore, outlines cell culture using a multilayer cell culture flask, which can handle the same number of cells as 10 traditional 175  $\text{cm}^2$  flasks.

## 2. Preparation of collagen-based scaffolds

NOTE: Coll-I-nHA and Coll-I-GAG cylindrical scaffolds (diameter 6 mm, height 4 mm) are prepared using established methods<sup>15,21,27</sup>. Once chemically crosslinked as per previously published methods<sup>17</sup>, the scaffolds must be used within 1 week.

2.1. Following the manufacture of the scaffolds with the desired mechanical properties, ensure that the scaffolds are fully hydrated and thoroughly washed in phosphate-buffered saline (PBS).

NOTE: This generally takes ~12 h after the crosslinking of the scaffolds and can be carried out in 100 mL tissue culture waste containers at 4 °C, with a maximum of 50 scaffolds per container and 2 mL of PBS per scaffold.

2.2. Store the scaffolds in PBS at 4 °C until ready to use.

### 3. Propagate neuroblastoma cells in a multilayer cell culture flask

NOTE: The optimal seeding density for the multilayer flask will vary. For the flask used in this experiment, the optimal density as per the manufacturer's instructions is  $1 \times 10^7$  cells. Before seeding the multilayer flask, propagate cells to a density of  $1 \times 10^7$  cells or higher in an appropriate tissue culture flask (e.g., a T175 cm<sup>2</sup> tissue culture flask). To seed cells into the multilayer flask (section 3.1), grow them until 70–80% confluent, harvest, and count the numbers of cells per mL, referring to steps 3.2.16–3.2.20 for performing the cell count. Once the cell suspension is counted, proceed immediately to the seeding of the multilayer flask. Cell culture work must be carried out in a laminar flow hood to maintain sterility.

#### 3.1. Seeding the multilayer cell culture flask

3.1.1. Prewarm 550 mL of complete growth medium (varies depending on the cell line in use) and 100 mL of sterile PBS in a 37 °C water bath for 20 min.

3.1.2. Using the harvested cell suspension, calculate the required volume of the cell suspension needed to achieve the optimal seeding density of  $1 \times 10^7$  cells using equation (1), where WANT refers to the number of cells required for seeding the multilayer flask, and HAVE refers to the number of cells/mL in the cell suspension:

$$\frac{WANT \text{ (cells per mL)}}{HAVE \text{ (cells per mL)}} \times 1000 \mu\text{L} = \text{required volume of cell suspension} \quad (1)$$

$$\text{e.g., } \frac{1 \times 10^7}{2 \times 10^7} \times 1000 \mu\text{L} = 500 \mu\text{L cell suspension required}$$

3.1.3. Add the required volume of the cell suspension to 100 mL of the prewarmed growth medium.

3.1.4. Take a new multilayer flask in the hood, remove the cap, and hold the flask at a 60° angle. Slowly pipette all 100 mL of the cell suspension into the flask, down the angled side of the neck. Cap the flask and place it on its side to allow the cells to distribute throughout the layers evenly.

3.1.5. At a 60° angle, add 400 mL of the prewarmed growth medium to the multilayer flask by slowly pouring or pipetting down the angled side of the neck. If the neck becomes full, return the flask to an upright position, or cap the flask and place it on its side before returning to pouring.

NOTE: Pour slowly to avoid excessive bubble formation. Gently tap the flask in the upright position to allow all bubbles to rise to the top and remove them with a 10 mL pipette. Ensure the flask is filled to the bottom thread of the neck; add more medium, if necessary, to achieve this.

3.1.6. Cap the multilayer flask and incubate it with the angled neck facing down at 37 °C, 5% CO<sub>2</sub>, and 95% humidity.

3.1.7. Check the growth every 2–3 days for confluency. To check the confluency of the bottom two layers of the multilayer flask, view them under a 4x objective lens of an inverted microscope.

NOTE: When seeded with  $1 \times 10^7$  neuroblastoma cells, the 10-layer flask will typically take one week to become confluent—though this may vary depending on the cell line used.

### 3.2. Routine maintenance of cells in the multilayer flask

3.2.1. Prewarm 550 mL of complete growth medium (varies depending on the cell line in use), 50–100 mL of trypsin, and 300 mL of sterile PBS in a 37 °C water bath for 20 min.

3.2.2. Check the multilayer flask for 70–80% confluency.

3.2.3. Place the multilayer flask in a laminar flow hood and discard the spent medium from the flask by pouring. Initially, tilt the flask so that the medium is pouring over the air dam into a waste container. While pouring, rotate the flask by 180° until the medium is flowing down the angled neck of the flask. Rotate the flask back and forth along this axis to eliminate any remaining liquid.

3.2.4. Wash the cells by adding 100 mL of prewarmed sterile PBS slowly down the angled neck. Cap the flask, place it on its side to allow uniform distribution of PBS, and rotate the flask back and forward to wash the cells.

3.2.5. Discard the PBS wash in the same manner as 3.2.3. Repeat the washing steps.

3.2.6. Dilute 50 mL of the prewarmed trypsin in 50 mL of prewarmed sterile PBS. Add 100 mL of diluted trypsin solution to the multilayer flask, cap, and place the flask on its side to allow uniform distribution of the trypsin. If the cell line is highly adherent, use 100 mL of undiluted trypsin.

3.2.7. Incubate the flask for 2–5 min at 37 °C, 5% CO<sub>2</sub>, and 95% humidity, monitoring cell detachment under the microscope. If necessary, tap the flask firmly to aid detachment or place it back in the incubator for one more minute.

3.2.8. Place the multilayer flask in a laminar flow hood and neutralize the trypsin with 100 mL of growth medium. Cap the flask, place it on its side, and rock back and forward to ensure complete neutralization.

3.2.9. Pour off the neutralized cell suspension into 4 x 50 mL conical centrifuge tubes.

NOTE: If complete cell harvest is required, wash the multilayer flask again with 100 mL of sterile PBS and pour it off into 2 x 50 mL centrifuge tubes.

3.2.10. Centrifuge the cell suspension in 50 mL centrifuge tubes at  $340 \times g$  for 3–4 min to pellet the cells.

3.2.11. Return the centrifuge tubes to the laminar flow hood and carefully discard as much supernatant as possible from each pellet.

NOTE: The pellet will be large and relatively loose and hence, can be disrupted easily.

3.2.12. Add 1–5 mL of growth medium to each pellet and resuspend it by pipetting up and down several times.

3.2.13. Pool together the 4 resuspended pellets in one 50 mL centrifuge tube, mix them thoroughly with the pipette, and note the total volume.

3.2.14. Make an appropriate dilution of the cell suspension for cell counting so that each outer square on the hemocytometer contains 30–100 cells.

NOTE: A suitable starting dilution is 1:100; for this, pipette 10  $\mu\text{L}$  of the cell suspension into a fresh 15 mL conical centrifuge tube and dilute it with 990  $\mu\text{L}$  of sterile PBS. Pipette the mixture up and down several times to mix thoroughly.

3.2.15. Place a 50 mL centrifuge tube containing the cell stock in the incubator while counting.

3.2.16. Taking a clean hemocytometer, place a clean coverslip over the grid, as shown in **Figure 2**.

3.2.17. Pipette 10  $\mu\text{L}$  of the diluted cell suspension into the hemocytometer chamber. If the chamber becomes full before all of the 10  $\mu\text{L}$  is dispensed, stop pipetting.

3.2.18. Place the hemocytometer under the 4x objective of a light microscope. Adjust the coarse and fine focus to visualize the cells.

3.2.19. Count the number of cells in the four outer corner squares of the chamber as highlighted in **Figure 2**. Add the four counts and divide by 4 to calculate the average cells per square.

[PLACE FIGURE 2 HERE]

3.2.20. Multiply the average count by the dilution factor (e.g., 100) and multiply this number by 10,000 to obtain the number of cells per mL using equation (2).

$$\frac{Square1+Square2+square3+Square4}{4} \times Dilution Factor \times 10,000 = cells per mL \quad (2)$$

3.2.21. Calculate the total number of cells in the stock solution by multiplying by the total volume of the cell stock (e.g., if the 4 resuspended pellets pooled made a 20 mL solution, multiply cells/mL by 20).

3.2.22. To maintain the multilayer flask, use equation (1) outlined in step 3.1.2 to calculate the volume of cell stock needed to seed  $1 \times 10^7$  cells back into the flask and carry out steps 3.1.3–3.1.6 to re-seed the flask. If ready to seed the scaffolds, proceed to the next section.

#### 4. Seed neuroblastoma cells on scaffolds

##### 4.1. Prepare stock cell suspension

NOTE: This protocol will outline the steps for creating four different seeding densities of neuroblastoma cells, with a multiplication factor of 2 between each density. A serial dilution will therefore be used to create three further cell suspensions from the stock suspension. Cell culture work must be carried out in a laminar flow hood to maintain sterility.

4.1.1. Use equation (3) to calculate the volume of cells needed from the total number of cells in the multilayer flask (counted in section 3.2.19) to prepare the first seeding density or cell stock suspension.

$$\frac{WANT (cells per mL)}{HAVE (cells per mL)} \times Required Volume (\mu L) = Volume of cells needed \quad (3)$$

NOTE: For example, if the highest seeding density is  $6 \times 10^5$  cells per scaffold required for 30 scaffolds, with each scaffold receiving 20  $\mu L$  of cell suspension, the stock cell suspension would require  $1.8 \times 10^7$  cells ( $6 \times 10^5$  cells  $\times$  30 scaffolds) in a total volume of 600  $\mu L$  (20  $\mu L \times$  30 scaffolds). As a serial dilution will be performed from this preparation, these numbers must be doubled, i.e.,  $3.6 \times 10^7$  cells in a total volume of 1200  $\mu L$ . To convert this to WANT in cells per mL; divide  $3.6 \times 10^7$  by 1200  $\mu L$  and multiply by 1000  $\mu L$ , giving  $3 \times 10^7$  cells per mL.

$$\frac{WANT (3 \times 10^7 cells per mL)}{HAVE (cells per mL from cell count)} \times 1200 \mu L = Cell Stock Required (mL)$$

4.1.2. Add the required volume of cell stock to a sterile 2 mL or 15 mL centrifuge tube and bring to a final volume of 1200  $\mu L$  with growth medium. Label this tube as **Density 1 (Figure 3)**.

4.2. Perform serial dilution to create multiple seeding density cell suspensions.

4.2.1. From **Density 1** prepared in step 4.1.1, prepare three more densities of cell suspension through serial dilution as per **Figure 3**.

4.2.2. Dilute each density by a factor of 2 in the growth medium. First, add the required final volume (600  $\mu$ L from the previous example) of growth medium to three sterile 2 mL or 15 mL centrifuge tubes.

4.2.3. Transfer half of **Density 1** (600  $\mu$ L) to one of the tubes, thoroughly mixing the cell suspension with the medium to dilute. Label this tube as **Density 2**.

4.2.4. Transfer half of **Density 2** (600  $\mu$ L) to the next tube, thoroughly mixing the cell suspension with the medium to dilute. Label this tube as **Density 3**.

4.2.5. Transfer half of **Density 3** (600  $\mu$ L) to the next tube, thoroughly mixing the cell suspension with the medium to dilute. Label this tube as **Density 4**.

4.2.6. Discard 600  $\mu$ L from **Density 4** so that all four preparations have a final volume of 600  $\mu$ L.

4.2.7. As a negative control, add 600  $\mu$ L of growth medium only to a sterile 2 mL centrifuge tube. See **Figure 3** for a schematic of the serial dilution process.

[PLACE **FIGURE 3** HERE]

#### 4.3. Adding cell suspensions to the scaffolds

NOTE: Remove the scaffolds (stored in PBS) from the refrigerator and allow them to come to room temperature (RT) before adding the cells.

4.3.1. Bring the scaffolds in PBS into the laminar flow hood.

4.3.2. Using sterile tweezers, place the scaffolds in non-adherent 24-well plates with one scaffold per well (**Figure 1C**). Gently lift the scaffolds by their corners and lightly press them against the side of the container to remove excess PBS. Add the scaffolds into the center of the wells skin-side-down (the shiny layer side of the scaffold, facing down into the plastic 24-well plates).

4.3.3. Label the 24-well plates with details of the cell line, relevant parameters (e.g., seeding density), and time points. Work with one cell seeding density at a time, keeping the remaining densities in the 37 °C incubator until ready for use.

4.3.4. In the laminar flow hood, use a P20 pipette and sterile tips to gently add 20  $\mu$ L of the relevant cell suspension to the center of each scaffold (**Figure 1D**). Keep the cells thoroughly in suspension by mixing well while adding the cells to the scaffolds. Ensure that the suspension remains on top of the scaffold and does not slide off onto the base of the well, as this will not allow cell attachment to the scaffold.

4.3.5. Once the cells have been added, incubate the plates for 3–5 h (37 °C, 5% CO<sub>2</sub>, and 95% humidity) to allow most of the cells to attach.

4.3.6. After incubation, slowly and gently add 1 mL of prewarmed growth medium to each well (**Figure 1E**). Use a P1000 pipette to add the medium to allow for more slow and controlled motion, preventing displacement of the scaffolds. If working with a very high number of scaffolds, use a 10 mL pipette with the pipette gun set to 'drop' and 'low.'

4.3.7. Incubate the 24-well plates overnight (37 °C, 5% CO<sub>2</sub>, and 95% humidity).

#### 4.4. Maintenance of cells on the scaffolds

4.4.1. After the first 24 h of cell attachment (Day 1), transfer the seeded scaffolds to new non-adherent 24-well plates, and add 1–2 mL of fresh growth medium.

NOTE: This step removes cells that have fallen to the bottom of the plastic 24-well plates rather than allowing them to grow on the scaffolds. Scaffold replicates designated as Day 1 will be taken down after 24 h, as discussed in section 5; hence, maintenance does not apply to these scaffolds.

4.4.2. Monitor the scaffolds initially every 2–3 days for a change in color of the growth medium. As time progresses and cells proliferate within the scaffolds, feed the cells more frequently.

4.4.3. Using a 10 mL pipette gun, on slow mode, remove the 1 mL of the spent medium and discard. If carrying out experiments requiring conditioned medium, collect the spent medium of biological replicates in a 15 mL centrifuge tube, centrifuge at  $340 \times g$  for 2 min to pellet the cellular debris, transfer the supernatant to a fresh tube, and store at –80 °C.

4.4.4. Gently add 2 mL of prewarmed growth medium to the scaffolds, using the drip function again on the pipette, and return the 24-well plate to the incubator (37 °C, 5% CO<sub>2</sub>, and 95% humidity). Repeat whenever the medium is spent for the duration of the desired growth period.

### 5. Scaffold retrieval and applications

NOTE: At each time point, several applications can be used to monitor cell growth on the scaffolds or assess gene and protein expression profiles. The conditions of scaffold retrieval will depend on the analysis to be performed, with multiple retrieval methods outlined in the following subsections and demonstrated in **Figure 4**.

#### 5.1. Assessment of cell viability within scaffolds

5.1.1. Sterilize the appropriate cell viability assay reagent by filtering through a 0.2 µm sterile filter into a centrifuge tube in the laminar flow hood. Prewarm this sterile solution along with complete growth medium and sterile PBS in a 37 °C water bath.



5.1.2. In the laminar flow hood, use sterile tweezers to transfer the scaffolds to be analyzed to a fresh 24-well plate. Label the plate with all relevant details.

NOTE: Perform the analysis in triplicate.

5.1.3. Add 900  $\mu$ L of the prewarmed growth medium to each well, followed by 100  $\mu$ L of the sterile cell viability reagent. Include a negative control by adding 900  $\mu$ L of medium and 100  $\mu$ L of the sterile cell viability reagent to a well with no scaffold. Replace the lid on the plate, and gently rock the plate for ~3 min to evenly distribute the diluted cell viability reagent throughout the well. Incubate the plate at 37 °C, 5% CO<sub>2</sub>, and 95% humidity.

NOTE: Incubation times will need to be optimized for each cell line; refer to the manufacturer's guidelines. For neuroblastoma cell lines, 4–6 h incubation appears optimal.

5.1.4. After incubation, remove the plate from the incubator and gently rock it for a few seconds.

5.1.5. In the laminar flow hood, open a new, translucent 96-well plate. From each well in the 24-well plate, transfer the incubated medium and reagent to three wells of the 96-well plate with 100  $\mu$ L per well, giving technical triplicates.

NOTE: This transfer will leave 700  $\mu$ L in the wells of the 24-well plate.

5.1.6. Cover the 96-well plate in aluminum foil to protect the cell viability reagent from light.

5.1.7. Remove and discard the remaining 700  $\mu$ L of the well contents from each scaffold in the 24-well plate. Wash each scaffold twice with 1 mL of sterile PBS.

NOTE: All color will not be removed from the scaffolds. These scaffolds can then be used for further applications, e.g., DNA quantification, by placing them in 1 mL of 1% Triton X-100 in 0.1 M sodium bicarbonate (NaHCO<sub>3</sub>) solution and storing them at –80 °C (see section 5.2, **Figure 4B**).

5.1.8. Remove the 96-well plate from the laminar flow hood and measure the absorbance of each well at wavelengths of 570 nm and 600 nm using a microplate reader. Record the absorbance values at both wavelengths and follow the manufacturer's instructions to calculate the percentage reduction of the cell viability reagent by the cells.

5.1.9. Graph and statistically analyze the cell viability results using appropriate software. Input biological triplicate values to produce error bars and indicate the assay variability.

5.1.10. To examine changes in cell viability over the experimental timeframe, perform a one-way analysis of variance (ANOVA) test with multiple comparisons of the means using appropriate biostatistical software.

5.1.11. Indicate significant differences between the time points on graphs as ns ( $P>0.05$ ), \* ( $P\leq 0.05$ ), \*\* ( $P\leq 0.01$ ), \*\*\* ( $P\leq 0.001$ ), and \*\*\*\* ( $P\leq 0.0001$ ).

[PLACE FIGURE 4 HERE]

## 5.2. Quantification of DNA from the cells in the scaffolds

NOTE: As mentioned in the note after step 5.1.7, the retrieval of the scaffolds for DNA quantification involves placing the scaffolds into 2 mL centrifuge tubes containing 1 mL of 1% Triton X-100 in 0.1 M  $\text{NaHCO}_3$  solution followed by storage at  $-80^\circ\text{C}$ . Before DNA analysis can be performed, the cells must undergo three freeze-thaw cycles to lyse the neuroblastoma cells appropriately and release DNA for quantification.

5.2.1. Remove the samples previously stored in Triton X-100 from  $-80^\circ\text{C}$ . Leave the samples at RT for 1–3 h or until thawed.

5.2.2. Vortex the samples for 10–20 s, and place the samples back at  $-80^\circ\text{C}$  for 18–24 h or until completely frozen. Repeat this process for a total of three freeze-thaw cycles.

5.2.3. To maximize the DNA yield, use a tissue lyser to disrupt the cells in the scaffolds.

5.2.3.1. Place a metal bead in the 2 mL centrifuge tube containing a scaffold in Triton X-100, and place the tube within the adaptor to shake the sample at 50 oscillations/second for 2–3 min.

NOTE: Use round-bottom centrifuge tubes as the metal bead may become lodged in a tapered-bottom tube.

5.2.4. Quantify the DNA in the Triton X-100 solution by applying a fluorescent double-stranded DNA (dsDNA) stain and measure the emission using a microplate reader. Refer to the manufacturer's guidelines; dilute the samples appropriately in Tris-ethylenediamine tetraacetic acid (TE) buffer to prepare 8 dsDNA standards through serial dilution in TE buffer (**Figure 5**).

5.2.5. In black opaque 96-well plates, add 100  $\mu\text{L}$  of each standard or sample to the wells in technical triplicate.

5.2.6. Dilute the fluorescent dsDNA stain 200-fold in TE buffer and add 100  $\mu\text{L}$  to each standard/sample using a multichannel pipette. Cover the plate in tinfoil and incubate at RT for 5 min.

5.2.7. Measure and record the fluorescence of each well at 520 nm. Follow the manufacturer's guidelines to calculate the concentration of DNA in each sample.

NOTE: If the average concentration of DNA per cell is known for the cell line being used, DNA concentration values can be converted to cell numbers using equation (4).

$$\frac{\text{Sample DNA Concentration (ng per mL)}}{\text{Average Concentration of DNA per cell (ng)}} = \text{Number of Cells in Sample} \quad (4)$$

5.2.8. Graph and statistically analyze the DNA quantification results using appropriate software. Input biological triplicate values to produce error bars and indicate the assay variability.

5.2.9. To examine the changes in DNA concentration/cell numbers over the experimental timeframe, perform a one-way ANOVA test with multiple comparisons of the means using appropriate biostatistical software.

5.2.10. Indicate significant differences between time points on graphs as ns ( $P > 0.05$ ), \* ( $P \leq 0.05$ ), \*\* ( $P \leq 0.01$ ), \*\*\* ( $P \leq 0.001$ ), and \*\*\*\* ( $P \leq 0.0001$ ).

[PLACE FIGURE 5 HERE]

### 5.3. Preparation of scaffolds for histological staining

NOTE: Scaffolds can be fixed and stained for microscopy and imaging purposes either as whole scaffolds for immunofluorescence (IF) or as formalin-fixed paraffin-embedded (FFPE) slices for histological staining or immunohistochemistry (IHC). This allows the qualitative assessment of cell penetration and distribution within scaffolds and can be used to assess the expression of proteins.

5.3.1. Prepare a 10% paraformaldehyde (PFA) solution in PBS. Ensure that there is enough solution for a final volume of 500  $\mu\text{L}$  per scaffold.

5.3.2. Prewarm this solution at 37  $^{\circ}\text{C}$  and add 500  $\mu\text{L}$  to labeled 2 mL centrifuge tubes for scaffold retrieval.

5.3.3. Remove the scaffolds from the non-adherent 24-well plates (step 4.4.4) and place them in the laminar flow hood.

5.3.4. Using sterile tweezers, transfer the scaffolds to the labeled centrifuge tubes containing 10% PFA. Allow the scaffolds to fix in the PFA solution for 15 min. Neutralize the PFA by adding 500  $\mu\text{L}$  PBS to each tube and store at 4  $^{\circ}\text{C}$ .

5.3.5. To prepare the scaffolds for the Automatic Tissue Processor, remove them from 4  $^{\circ}\text{C}$  and use tweezers to place them in plastic cassettes labelled with all relevant details in pencil. Place all the cassettes in the metal container of the Tissue Processor.

5.3.6. Begin the 12-stage protocol on the Tissue Processor to fix, dehydrate, clear the scaffolds, and infiltrate them with paraffin overnight. Collect the cassettes containing the processed samples.

5.3.7. Next, embed the scaffolds in paraffin wax blocks to allow microtomy of the scaffolds into very thin slices for staining.

NOTE: It is especially important to consider the orientation of the scaffolds when removing them from the cassettes and embedding them in wax, as this will affect the angle at which the images are taken. This is important when assessing cell infiltration into the scaffolds.

5.3.8. Turn on the wax embedder and the cold plate; lift the lid to check the level of the wax. Refill if necessary.

5.3.9. Working with one sample at a time, open the cassette, remove the scaffold, and center it in the plastic mold.

5.3.10. Pour hot wax onto the sample, ensuring that correct orientation is maintained and adjusting with warm tweezers, if necessary, before the wax solidifies. Pour more wax to fill the mold.

5.3.11. Place the labeled cassette lid on top of the plastic mold and add wax on top. Place the mold on the cold plate to solidify the wax. Store overnight at 4 °C to ensure that the paraffin wax is fully solidified before microtomy.

5.3.12. To prepare for microtomy, turn on a 35 °C water bath, the drying plate, and the microtome.

5.3.13. Insert a blade in the holder and tighten the lever to secure it.

5.3.14. Set the trim and section thickness, generally 5 mm for scaffold sections.

5.3.15. Remove the FFPE scaffold from the mold, secure it in the holder on the front of the microtome, and carefully trim the excess wax around the edges of the sample before cutting sections.

5.3.16. Start cutting into the wax block by rotating the lever of the microtome, ensuring smooth motion.

5.3.17. Collect ribbon-like sections, around 3 scaffold sections at a time, and gently place them in the 35 °C water bath to remove wrinkles. Gently separate the sections while in the water bath using tweezers.

5.3.18. Using polysine-coated glass microscope slides, lift each section from the water bath so that the section sits in the center of the slide. Label each slide with a pencil.

5.3.19. Place the glass slides on the drying plate or in a 60 °C drying oven. Once dried, store them at 4 °C and proceed with the required histological or IHC stain.

#### 5.4. Retrieval of scaffolds for gene expression analysis

5.4.1. Remove the scaffolds from the non-adherent 24-well plates from the incubator (step 4.4.4) and place them in the laminar flow hood.

5.4.2. Using sterile tweezers, transfer the scaffolds to fresh labeled 2 mL centrifuge tubes.

5.4.3. In a fume hood, add 1 mL of a phenol/guanidine-based cell lysis reagent to each tube to lyse the cells in scaffolds and allow for recovery of high-quality RNA.

5.4.4. Store tubes at –20 °C until ready to perform RNA extraction using an appropriate kit. Using a standard reverse-transcription quantitative polymerase chain reaction (RT-qPCR)<sup>17</sup>, assess gene expression in the cells in the scaffolds.

#### REPRESENTATIVE RESULTS:

The collagen-based scaffold model described here has many applications ranging from studying neuroblastoma biology to the screening of anticancer therapeutics in an environment that is more physiologically similar to native tumors than conventional 2D cell culture. Before testing a given research question, it is crucial to obtain a complete characterization of cell attachment, proliferation, and infiltration within the desired experimental timeframe. The growth conditions will depend on the biology of each specific cell line. Importantly, several methods of cell growth assessment must be implemented to determine optimal conditions and robust performance.

Here, the viability of neuroblastoma cells grown on scaffolds was assessed using a colorimetric cell viability assay. This assay can be performed as frequently as desired throughout the experimental timeframe. For the described experiment, cell viability assessment was performed on days 1, 7, and 14 for two neuroblastoma cell lines, KellyLuc and IMR32, grown on Coll-I-nHA scaffolds at 4 different densities (**Figure 6**). Viability on Day 1 was set as a baseline to compare all subsequent measurements. The rate of reduction of the cell viability reagent is reflective of the cell biology and growth characteristics of individual cell lines, including their proliferation rates and metabolism. A correlation between the number of cells seeded on the scaffolds and the level of reduction was expected. In this experiment, the reduction of the cell viability reagent generally increased with each time point for both cell lines at all densities, as expected.

Each density was then assessed individually for both cell lines to compare the reduction across time points. One-way ANOVA with Tukey's multiple comparisons test was performed to detect significant differences in reduction between time points (**Figure 7**). For both cell lines and all seeding densities, there was a significant increase ( $P < 0.05$ ) in the reduction of the cell viability

reagent when comparing day 1 and day 14. This indicated a significant increase in metabolically active cells present on the scaffolds. This increase was not significant in all cases when assessing the 7-day intervals (day 1 vs. day 7, day 7 vs. day 14), demonstrating the importance of the optimization of the seeding density to achieve the desired growth window.

To support the results of the cell viability assay, cell growth on scaffolds can also be indirectly measured via the quantification of dsDNA extracted from scaffolds using a fluorescent dsDNA stain (**Figure 8A**). Like cell viability, DNA quantification can be done as frequently as desired within the experimental timeline. However, this analysis requires the complete retrieval of scaffolds and termination of cell growth and so must be factored into experimental planning as discussed in section 1. For this experiment, DNA was quantified on days 1, 7, and 14 for two neuroblastoma cell lines, KellyLuc and IMR32, grown on Coll-I-nHA scaffolds at 4 different densities. As the average concentration of dsDNA per cell is known for these cell lines, it was possible to derive the number of cells per sample from the quantified DNA (**Figure 8B**).

DNA quantification gave rise to higher variability between biological replicates than cell viability assessment but generally increased for each time point, with the highest levels quantified on day 14. IMR32 cells appear to reach higher cell numbers on Coll-I-nHA scaffolds, as indicated by DNA concentration, than KellyLuc cells. Each density was then assessed individually for the two cell lines to compare the reduction across time points. One-way ANOVA with Tukey's multiple comparisons test was performed to detect significant differences in reduction between time points (**Figure 8B**).

For both cell lines and all seeding densities, there was a significant increase ( $P < 0.05$ ) in cell numbers when comparing day 1 and day 14, with the exception of KellyLuc at seeding density 4 ( $1 \times 10^5$  cells/scaffold), which did not yield significant increases across any of the time points. Similar to the cell viability results, the increases were not significant in all cases when assessing the 7-day intervals (day 1 vs. day 7, day 7 vs. day 14). When comparing the time point trends for cell viability and DNA quantification, there were some slight differences between the two analyses. However, overall similar trends were observed, with mean values increasing between 7-day intervals for most densities. This demonstrates the importance of monitoring cell growth using more than one method.

A visual assessment of cell growth morphology and distribution on the scaffolds was next implemented, encompassing traditional hematoxylin and eosin (H&E) staining as well as IHC. It is expected that the different growth patterns of individual cell lines will lead to varied spatial arrangements on scaffolds, including different degrees of penetration into the scaffold and cell clustering. Scaffolds were formalin-fixed, paraffin-embedded, and cut into 5 mm sections (**Figure 9A**), preparing the scaffolds for multiple visualization techniques, including histological staining and IHC.

Routine H&E staining was applied to Kelly, KellyCis83, and IMR32 cells grown on collagen-based scaffolds on days 1, 7, and 14 (**Figure 9B**). This allowed visualization of the cells' spatial orientation on two collagen-based scaffolds over a 14-day period. Cisplatin-sensitive Kelly cells

and resistant KellyCis83 cells were grown on both Coll-I-nHA scaffolds (**Figure 9B**, i) and Coll-I-GAG scaffolds (**Figure 9B**, ii). Consistent with previously published data, KellyCis83 cells grew at a higher rate and infiltrated deeper into both scaffold compositions than the less invasive Kelly cell line. The H&E stain of another neuroblastoma cell line, IMR32, grown on Coll-I-nHA demonstrates a contrasting growth pattern (**Figure 9B**, iii). This cell line grew in large, densely packed clusters on the collagen scaffolds over the 14-day period. Brightfield confocal microscopy can be used to visualize the porous architecture of collagen-based scaffolds (**Figure 9C**) owing to the autofluorescence of collagen fibers.

We stained cells with phalloidin targeting cytoskeletal actin and the nuclear counterstain, 4',6-diamidino-2-phenylindole (DAPI), to monitor specific cell traits throughout the experimental timeline. An abundance of actin was observed in Kelly and KellyCis83 cells on Coll-I-GAG scaffolds using this technique (**Figure 9D**). These results demonstrate how multiple imaging techniques can be used to derive spatially resolved information from neuroblastoma cells grown on scaffolds using this protocol. This characterization of cell growth patterns on collagen-based scaffolds over a given period will improve the understanding and interpretation of any downstream biochemical assays.

Protein expression by cells grown on collagen-based scaffolds can be analyzed to compare cellular activity to *in vivo* scenarios. Previously published data examined the expression of chromogranin A (CgA) as a surrogate secreted marker of neuroblastoma by KellyLuc and KellyCis83Luc cells grown in cell monolayers as well as on Coll-I-nHA and Coll-I-GAG scaffolds (**Figure 10**). CgA was assessed in the conditioned media using an enzyme-linked immunosorbent assay (ELISA) (**Figure 10A**). CgA is secreted at a higher rate in the more aggressive chemo-resistant KellyCis83 cell line than in Kelly (**Figure 10B,C**). This was significant on day 7 on both Coll-I-GAG and Coll-I-nHA scaffolds ( $P < 0.05$ ), whereas there was no significant difference at this time point for cells grown as a monolayer by conventional 2D culture.

These results also highlight the restricted experimental timeline when growing cells in a monolayer, with only 7 days of growth proving feasible before cells reach confluency. The growth of cells on scaffolds overcomes this limitation as they can be maintained over a longer period in more physiologically relevant conditions. The above combination of techniques to acquire information on cell viability, DNA content, cellular morphology and spatial arrangement, and expression profiles facilitates the assessment of the growth of neuroblastoma cells on a range of collagen-based scaffolds. This protocol can also be easily adapted to satisfy specific experimental requirements and desired applications.

[PLACE FIGURE 6 HERE]

[PLACE FIGURE 7 HERE]

[PLACE FIGURE 8 HERE]

[PLACE FIGURE 9 HERE]

[PLACE FIGURE 10 HERE]

#### FIGURE AND TABLE LEGENDS:

**Figure 1: Overall protocol workflow.** (A) Cells are grown to sufficient numbers, split, counted, and resuspended in an appropriate volume of medium. (B) This cell stock then undergoes serial dilution to prepare a total of 4 cell suspensions of different densities. (C) Collagen-based scaffolds are sterilely plated in non-adherent 24-well plates, and (D) 20  $\mu\text{L}$  of cell suspension is added to the center of each scaffold and left to incubate at 37  $^{\circ}\text{C}$ , 5%  $\text{CO}_2$ , and 95% humidity for 3–5 h. (E) Complete growth medium (1 mL) is then slowly added to each scaffold, and the plates are placed back into the incubator to allow cell growth for the desired timeframe. (F) At each predetermined time point, several scaffolds are retrieved for cell viability and growth assessment, gene expression analysis, and histological staining.

**Figure 2: Cell counting using a hemocytometer.** Ten microliters of cell suspension are added to the hemocytometer beneath the coverslip. The chamber is then placed under the 4x objective lens of a microscope, and the number of cells in the four outer corners of the grid are counted.

**Figure 3: Serial dilution of cell stock to prepare 4 suspensions for 4 different scaffold seeding densities.** (A) Numbers can be adjusted to suit the desired seeding density per scaffold and (B) multiplied for the total number of scaffolds per density, with each scaffold receiving 20  $\mu\text{L}$  of cell suspension. In this example, Density 1 requires  $6 \times 10^5$  cells per scaffold, equivalent to  $1.8 \times 10^7$  cells in 600  $\mu\text{L}$  for 30 scaffolds. This number is doubled to begin the serial dilution, as 600  $\mu\text{L}$  is then transferred and diluted in 600  $\mu\text{L}$  of growth medium in the next tube. This process continues until there are 4 cell suspensions with a factor of 2 between each. A negative control is made by adding 600  $\mu\text{L}$  of medium only to a tube.

**Figure 4: Retrieval of scaffolds for different analyses at each time point.** (A) Three scaffold replicates are retrieved for cell viability analysis. (B) These scaffolds can then be washed in PBS, placed in 1% Triton X-100 in 0.1 M  $\text{NaHCO}_3$ , and stored at  $-80^{\circ}\text{C}$  for DNA quantification. (C) Three more replicates are fixed in 10% PFA for 15 min, neutralized in PBS, and stored at 4  $^{\circ}\text{C}$  for histological staining and imaging. (D) Finally, 3 replicates are added to a phenol/guanidine-based cell lysis reagent and stored at  $-20^{\circ}\text{C}$  for gene expression analysis. Abbreviations: PBS = phosphate-buffered saline; PFA = paraformaldehyde.

**Figure 5: Preparation of eight DNA standards for the generation of a standard curve.** A stock solution of  $\lambda\text{DNA}$  is provided at 100  $\mu\text{g}/\text{mL}$ . This is diluted 50-fold in TE buffer to create standard A at 2000  $\text{ng}/\text{mL}$ ; 400  $\mu\text{L}$  of A is then transferred to tube B, containing 400  $\mu\text{L}$  TE buffer; 400  $\mu\text{L}$  of B is then transferred and diluted 2-fold in C, and so on until G. Standard H is composed of only TE buffer and therefore has a DNA concentration of 0  $\text{ng}/\text{mL}$ . Abbreviation: TE = Tris-EDTA.



**Figure 6: Cell viability analysis.** (A) General procedure for measuring the viability of neuroblastoma cells on collagen-based scaffolds using a colorimetric cell viability assay. The incubation period must be optimized for each new cell line, referring to the manufacturer's guidelines. (B) Percentage reduction of cell viability reagent by KellyLuc and IMR32 cells grown on Coll-I-nHA scaffolds at four different initial seeding densities, measured on days 1, 7, and 14. Samples were assessed in biological triplicate with error bars representing the standard deviation. Abbreviations: nHA = nanohydroxyapatite; Coll-I-nHA = collagen scaffolds supplemented with nHA.

**Figure 7: Cell viability by seeding density for cells grown on Coll-I-nHA over a 14-day period.** (A) KellyLuc; (B) IMR32. Titled cell numbers refer to the initial cell seeding density on the scaffolds on Day 0. Samples were assessed in biological triplicate, indicated by triplicate points, with bars representing the mean. One-Way ANOVA with Multiple Comparisons was used to detect significant differences in % cell viability reagent reduction across the three time points, noted on the graphs (ns  $P > 0.05$ , \*  $P \leq 0.05$ , \*\*  $P \leq 0.01$ , \*\*\*  $P \leq 0.001$ , \*\*\*\*  $P \leq 0.0001$ ). Abbreviations: nHA = nanohydroxyapatite; Coll-I-nHA = collagen scaffolds supplemented with nHA; ANOVA = analysis of variance; ns = not significant.

**Figure 8: Quantification of DNA extracted from cells in scaffolds.** (A) Process of quantifying dsDNA from cells grown on collagen-based scaffolds using a fluorescent dsDNA stain. (B) Cell numbers from DNA quantification analysis by seeding density for KellyLuc and IMR32 cells grown on Coll-I-nHA over a 14-day period. Titled cell numbers refer to the initial cell seeding density onto scaffolds on Day 0. Samples were assessed in biological triplicate, indicated by triplicate points, with bars representing the mean. One-Way ANOVA with Multiple Comparisons was used to detect significant differences in cell numbers across the three time points, noted on the graphs (ns  $P > 0.05$ , \*  $P \leq 0.05$ , \*\*  $P \leq 0.01$ , \*\*\*  $P \leq 0.001$ , \*\*\*\*  $P \leq 0.0001$ ). Abbreviations: nHA = nanohydroxyapatite; Coll-I-nHA = collagen scaffolds supplemented with nHA; dsDNA = double-stranded DNA; TE = Tris-EDTA; ANOVA = analysis of variance; ns = not significant.

**Figure 9: Tissue processing steps for immunohistochemistry analysis of scaffolds.** (A) Schematic representation of the protocol for processing scaffolds for image analysis. This process allows routine histological staining and specific antibody probing using primary antibodies and fluorescently labeled secondary antibodies. (B) Representative images of three neuroblastoma cell lines subjected to H&E staining. H&E images are taken on Days 1, 7, 14 to monitor growth patterns over the time course of the experiment. Scale bar = 200  $\mu\text{m}$ . Dashed squares represent the area that was chosen for zoomed-in 20x images at the lower left edge. Scale bar = 20  $\mu\text{m}$ . (i and ii) H&E of Kelly and KellyCis83 neuroblastoma cell lines (upper and lower panels, respectively) on two types of collagen-based scaffolds. (iii) H&E of IMR32 cell line, representing clustered cellular growth on the Coll-I-nHA scaffold. (C) Representative image of the Kelly cell line, subjected to brightfield confocal microscopy. The collagen autofluorescence allows visualization of the porous scaffold. 10x Scale bar = 200  $\mu\text{m}$ , 20x scale bar = 20  $\mu\text{m}$ . (D) Representative image of embedded scaffolds followed by analysis by IHC with phalloidin and DAPI at 10x magnification, Scale bar = 200  $\mu\text{m}$ . Smaller inside squares represent zoomed-in images (20x), scale bar = 20  $\mu\text{m}$ .

Abbreviations: nHA = nanohydroxyapatite; Coll-I-nHA = collagen scaffolds supplemented with nHA; GAG = glycosaminoglycan; Coll-I-GAG = collagen scaffolds supplemented with chondroitin-6-sulfate; H&E = hematoxylin and eosin; IHC = immunohistochemistry; DAPI = 4',6-diamidino-2-phenylindole.

**Figure 10: Protein expression by neuroblastoma cells grown on 3D collagen-based scaffolds compared to 2D plastic.** (A) A schematic of how the CgA ELISA was performed on conditioned media of cells grown on 2D plastic or 3D collagen-based scaffolds. (B) CgA protein expression levels taken from conditioned media of cells grown on a 2D plastic monolayer. As the cells reached confluency after 7 days, the 14-day time point was not readable. By day 7 on plastic, there was no significant difference in CgA levels between Kelly and KellyCis83 cell lines. (C) CgA ELISA performed using conditioned media of cells grown on collagen-based scaffolds for 14 consecutive days. On day 7, on both collagen scaffolds, CgA levels are higher in the more aggressive KellyCis83 cell line, highlighting more physiological relevant levels of CgA in 3D matrix compared to 2D monolayer. This figure has been modified from Curtin et al.<sup>17</sup>. Abbreviations: 3D = three-dimensional; 2D = two-dimensional; CgA = chromogranin A; ELISA = enzyme-linked immunosorbent assay; nHA = nanohydroxyapatite; Coll-I-nHA = collagen scaffolds supplemented with nHA; GAG = glycosaminoglycan; Coll-I-GAG = collagen scaffolds supplemented with chondroitin-6-sulfate; TMB = 3,3',5,5'-tetramethylbenzidine; HRP = horseradish peroxidase.

**Table 1: Overview of the mechanical properties of the two scaffolds adopted for studying neuroblastoma biology.**

## DISCUSSION:

The 3D scaffold–cancer cell model has been proven as a valuable and versatile tool for gaining mechanistic insight into neuroblastoma cell growth, viability, and infiltration of cells in a simplified TME<sup>32</sup>. The 3D neuroblastoma model described here mimics the minimal TME and provides more physiologically relevant data than a 2D monolayer culture. A major drawback of 3D cell culture is increased experimental complexity and longer timeframes. Described here is an optimized protocol for seeding, growth, and maintenance of neuroblastoma cells on collagen-based scaffolds followed by downstream analyses and applications, yielding robust characterization of cell growth. We aimed to gain insights into the optimal cell seeding density for the scaffolds to create a predictable and controllable environment for assessing anticancer drug treatments in an expeditious 14-day experimental window. The combination of all these described simple protocols provides a well-rounded assessment of neuroblastoma cell growth in the scaffold-based *in vitro* culture system.

The critical points in the protocol setup have been emphasized to allow scientists to establish the same in their laboratories quickly. For example, the indicated incubation times for better performance of the colorimetric cell viability assay allow deeper penetration of the reagent into the scaffold pores to reach all cells. Moreover, the fluorescent dsDNA staining technique is robust and straightforward; however, DNA release from the scaffolds requires vigorous cell lysis as the cells are ‘trapped’ within collagen fibers.

Using the simple DNA quantification assay described, we can identify the log growth phase on collagen-based scaffolds for anticancer drug screening using this model. In the described experimental setting, 4 initial cell seeding densities were used with an overall 14-day period and analysis time points on Days 1, 7, and 14. We identified that KellyLuc cells seeded at  $4 \times 10^5$  cells/scaffold have the most significantly active proliferation window between Days 7 and 14. This log phase growth data will allow for reliable interpretation of various cell cytotoxicity experiments. It eliminates speculation about any decline in growth or cell death resulting from suppressed growth on the 3D porous platform rather than from drug toxicities. Cell viability is also a widely used assessment for the suitability of 3D platforms to support the growth of different cell types<sup>33,34</sup>. While there are many assays to measure cell viability, including live/dead staining, ATP measurement, proliferation assays, we found the use of the Alamar Blue colorimetric cell viability assay to be a simple and effective technique to support DNA quantification data.

The combined use of DNA quantification and cell viability provided complementary evidence that, on average, the optimal density to seed cells on the scaffold to achieve continued growth over a 14-day period is  $2\text{--}4 \times 10^5$  cells/scaffold. However, this protocol can easily be adapted to satisfy different experimental timeframes, analysis time points, and downstream applications. Although this protocol describes the evaluation of monoculture cell growth of neuroblastoma cells on scaffolds, the scaffolds are easily amendable for use as a platform for co-culture, described by do Amaral et al., who utilized collagen-GAG scaffolds to co-culture keratinocytes and fibroblasts in an investigation of wound healing<sup>35</sup>.

The described 3D model enables the visualization of cell growth and infiltration using different well-known techniques, such as immunofluorescence and standard H&E. It is important to visualize the cells along with the characterization of growth using biochemical assays due to the diversity of cell morphology and growth patterns on scaffolds. Understanding the growth pattern can yield insights into growth behavior and future response to anticancer drugs. For example, IMR32 growth using DNA quantification yields similar patterns to Kelly, although upon visualization using H&E, IMR32 grows in larger clusters than Kelly, which displayed more dispersed growth (**Figure 9**). These varied growth patterns of cell lines in scaffolds reflect the clinical scenario of tumor heterogeneity. Examining anticancer drug response using a panel of cell lines with different morphologies in 3D scaffolds will increase the predictive value for patient response to the same drugs.

Detection of gene or protein expression can also be performed using other approaches such as RT-qPCR or ELISA if the protein of interest is secreted. A surrogate marker of neuroblastoma progression, chromogranin A (CgA)<sup>36</sup>, was used to additionally characterize neuroblastoma cell growth in 3D. As described in previous work<sup>17</sup>, CgA secretion increased as cells proliferated (**Figure 10**). While monolayer cell culture could not capture this increase, as proliferation meant cells reached full confluency in the culture dishes, the use of the 3D collagen scaffolds allowed prolonged assessment of CgA secretion.

This 3D *in vitro* model may not be suitable for all research questions to study neuroblastoma biology and response to therapeutics. One of the limitations is uneven cell penetration within scaffolds and the formation of cell clusters of varying size, which depends on a given cell line and may lead to uncontrollable diffusion of nutrients and test drugs. This feature affects the robustness in therapeutic screening. However, despite this limitation, it is important to consider that native tumors are also heterogeneous in size and cancer cell distribution and contain many other cell types within the tumor tissue. To overcome this limitation, we propose the use of each cell-populated scaffold as a single microtissue for which the following parameters will be optimized: (a) incubation times for the cell viability reagent to reach the cells and cell clusters, and (b) lysing of the cells in Triton X-100 buffer by preprocessing of cells on scaffolds with a tissue lyser to release the DNA of the cells contained deep in the scaffold.

Another technical limitation of this protocol is the lack of mechanical testing of each batch of newly manufactured scaffolds for this model. However, using the robust manufacturing process of the scaffolds, which have been extensively characterized in relation to physical and chemical properties of the scaffolds, such as compressive and tensile modulus, porosity and visual pore structure, and homogeneity, ensures that scaffold qualities are maintained through batches<sup>21,24,27,30,37</sup>.

In summary, this paper presents a series of simple methods for the analysis of cellular growth on collagen-based scaffolds. Both the experimental timeline and analysis points can be interchanged depending on the specific research questions. This protocol is also adaptable to other cell types. The results shown above provide evidence on how this compilation of methods gave insight into the optimal seeding density for various neuroblastoma cell lines to create continuous growth over 14 days. The amalgamation of results obtained from all the methods in this protocol yields a superior understanding of cell growth within the 3D collagen matrix. Future utilization of this model will likely involve co-culture systems specific to the neuroblastoma TME and the testing of various novel anticancer drugs.

#### ACKNOWLEDGMENTS:

This work was supported by the National Children's Research Centre (NCRC), Irish Research Council (IRC), and Neuroblastoma UK. The illustrations were created using BioRender.

#### DISCLOSURES:

The authors declare no conflicts of interest.

#### REFERENCES:

1. Davidoff, A. M. Neuroblastoma. *Seminars in Pediatric Surgery*. **21** (1), 2–14 (2012).
2. Matthay, K. K. et al. Neuroblastoma. *Nature Reviews Disease Primers*. **2**, 16078 (2016).
3. Costard, L. S., Hosn, R. R., Ramanayake, H., O'Brien, F. J., Curtin, C. M. Influences of the 3D microenvironment on cancer cell behaviour and treatment responsiveness: a recent update on lung, breast and prostate cancer models. *Acta Biomaterialia*. doi:10.1016/j.actbio.2021.01.023 (2021).
4. Borriello, L., Seeger, R. C., Asgharzadeh, S., Declerck, Y. A. More than the genes, the tumor

- microenvironment in neuroblastoma. *Cancer Letters*. **380** (1), 304–318 (2016).
5. Walker, C., Mojares, E., Del Río Hernández, A. Role of extracellular matrix in development and cancer progression. *International Journal of Molecular Sciences*. **19** (10), 3028 (2018).
  6. Bissell, M. J., Hall, H. G., Parry, G. How does the extracellular matrix direct gene expression? *Journal of Theoretical Biology*. **99** (1), 31–68 (1982).
  7. Schultz, G. S., Davidson, J. M., Kirsner, R. S., Bornstein, P., Herman, I. M. Dynamic reciprocity in the wound microenvironment. *Wound Repair and Regeneration*. **19** (2), 134–148 (2011).
  8. Brancato, V., Oliveira, J. M., Correló, V. M., Reis, R. L., Kundu, S. C. Could 3D models of cancer enhance drug screening? *Biomaterials*. **232**, 119744 (2020).
  9. Provenzano, P. P. et al. Collagen density promotes mammary tumor initiation and progression. *BMC Medicine*. **6**, 11 (2008).
  10. Provenzano, P. P. et al. Collagen reorganization at the tumor-stromal interface facilitates local invasion. *BMC Medicine*. **4**, 38 (2006).
  11. Ouellette, J. N. et al. Navigating the collagen jungle: The biomedical potential of fiber organization in cancer. *Bioengineering*. **8** (2), 1–19 (2021).
  12. Kreger, S. T., Voytik-Harbin, S. L. Hyaluronan concentration within a 3D collagen matrix modulates matrix viscoelasticity, but not fibroblast response. *Matrix Biology*. **28** (6), 336–346 (2009).
  13. Frantz, C., Stewart, K. M., Weaver, V. M. The extracellular matrix at a glance. *Journal of Cell Science*. **123** (24), 4195–4200 (2010).
  14. Hume, R. D. et al. Tumour cell invasiveness and response to chemotherapeutics in adipocyte invested 3D engineered anisotropic collagen scaffolds. *Scientific Reports*. **8** (1), 12658 (2018).
  15. Fitzgerald, K. A. et al. The use of collagen-based scaffolds to simulate prostate cancer bone metastases with potential for evaluating delivery of nanoparticulate gene therapeutics. *Biomaterials*. **66**, 53–66 (2015).
  16. Sapudom, J., Pompe, T. Biomimetic tumor microenvironments based on collagen matrices. *Biomaterials Science*. **6** (8), 2009–2024 (2018).
  17. Curtin, C. et al. A physiologically relevant 3D collagen-based scaffold–neuroblastoma cell system exhibits chemosensitivity similar to orthotopic xenograft models. *Acta Biomaterialia*. **70**, 84–97 (2018).
  18. Gavin, C. et al. Neuroblastoma invasion strategies are regulated by the extracellular matrix. *Cancers*. **13** (4), 1–23 (2021).
  19. Ridky, T. W., Chow, J. M., Wong, D. J., Khavari, P. A. Invasive three-dimensional organotypic neoplasia from multiple normal human epithelia. *Nature Medicine*. **16** (12), 1450–1456 (2010).
  20. Casale, J., Crane, J. S. *Biochemistry, Glycosaminoglycans*. StatPearls Publishing, Treasure Island, FL, USA (2019).
  21. O’Brien, F. J., Harley, B. A., Yannas, I. V., Gibson, L. J. The effect of pore size on cell adhesion in collagen-GAG scaffolds. *Biomaterials*. **26** (4), 433–441 (2005).
  22. O’Brien, F. J., Harley, B. A., Yannas, I. V., Gibson, L. Influence of freezing rate on pore structure in freeze-dried collagen-GAG scaffolds. *Biomaterials*. **25** (6), 1077–1086 (2004).
  23. Haugh, M. G., Murphy, C. M., McKiernan, R.C., Altenbuchner, C., O’Brien, F. J. Crosslinking

and mechanical properties significantly influence cell attachment, proliferation, and migration within collagen glycosaminoglycan scaffolds. *Tissue Engineering. Part A*. **17** (9–10), 1201–1208 (2011).

24. Murphy, C. M., Haugh, M. G., O'Brien, F. J. The effect of mean pore size on cell attachment, proliferation and migration in collagen-glycosaminoglycan scaffolds for bone tissue engineering. *Biomaterials*. **31** (3), 461–466 (2010).

25. Haugh, M. G., Jaasma, M.J., O'Brien, F. J. The effect of dehydrothermal treatment on the mechanical and structural properties of collagen-GAG scaffolds. *Journal of Biomedical Materials Research - Part A*. **89A** (2), 363–369 (2009).

26. Lowe, B., Hardy, J. G., Walsh, L. J. Optimizing nanohydroxyapatite nanocomposites for bone tissue engineering. *ACS Omega*. **5** (1), 1–9 (2020).

27. Cunniffe, G. M., Dickson, G. R., Partap, S., Stanton, K. T., O'Brien, F. J. Development and characterisation of a collagen nano-hydroxyapatite composite scaffold for bone tissue engineering. *Journal of Materials Science. Materials in Medicine*. **21** (8), 2293–2298 (2010).

28. DuBois, S. G. et al. Metastatic sites in stage IV and IVS neuroblastoma correlate with age, tumor biology, and survival. *Journal of Pediatric Hematology/Oncology*. **21** (3), 181–189 (1999).

29. Ryan, A. J., Gleeson, J. P., Matsiko, A., Thompson, E. M., O'Brien, F. J. Effect of different hydroxyapatite incorporation methods on the structural and biological properties of porous collagen scaffolds for bone repair. *Journal of Anatomy*. **227** (6), 732–745 (2015).

30. Tierney, C. M. et al. The effects of collagen concentration and crosslink density on the biological, structural and mechanical properties of collagen-GAG scaffolds for bone tissue engineering. *Journal of the Mechanical Behavior of Biomedical Materials*. **2** (2), 202–209 (2009).

31. Cox, R. F., Jenkinson, A., Pohl, K., O'Brien, F. J., Morgan, M. P. Osteomimicry of mammary adenocarcinoma cells in vitro; increased expression of bone matrix proteins and proliferation within a 3D collagen environment. *PLoS One*. **7** (7), e41679 (2012).

32. Nolan, J. C. et al. Preclinical models for neuroblastoma: advances and challenges. *Cancer Letters*. **474**, 53–62 (2020).

33. Sirivisoot, S., Pareta, R., Harrison, B. S. Protocol and cell responses in threedimensional conductive collagen gel scaffolds with conductive polymer nanofibres for tissue regeneration. *Interface Focus*. **4**( 1), 20130050 (2014).

34. Thevenot, P., Nair, A., Dey, J., Yang, J., Tang, L. Method to analyze three-dimensional cell distribution and infiltration in degradable scaffolds. *Tissue Engineering. Part C-Methods*. **14** (4), 319–331 (2008).

35. do Amaral, R. J. F. C. et al. Functionalising collagen-based scaffolds with platelet-rich plasma for enhanced skin wound healing potential. *Frontiers in Bioengineering and Biotechnology*. **7**, 371 (2019).

36. Gkolfinopoulos, S., Tsapakidis, K., Papadimitriou, K., Papamichael, D., Kountourakis, P. Chromogranin A as a valid marker in oncology: Clinical application or false hopes? *World Journal of Methodology*. **7** (1), 9–15 (2017).

37. O'Brien, F. J. et al. The effect of pore size on permeability and cell attachment in collagen scaffolds for tissue engineering. *Technology and Health Care*. **15** (1), 3–17 (2007).

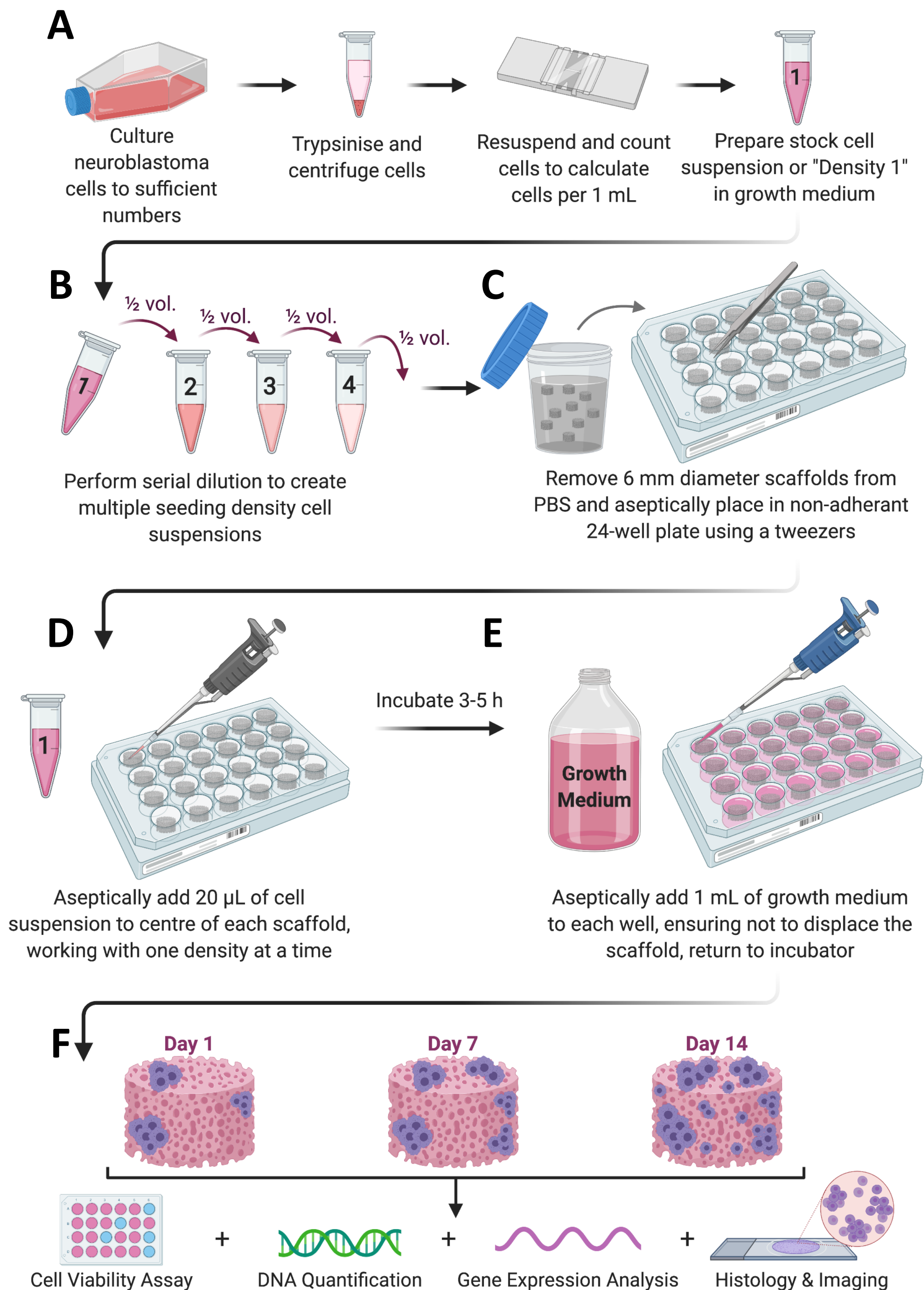
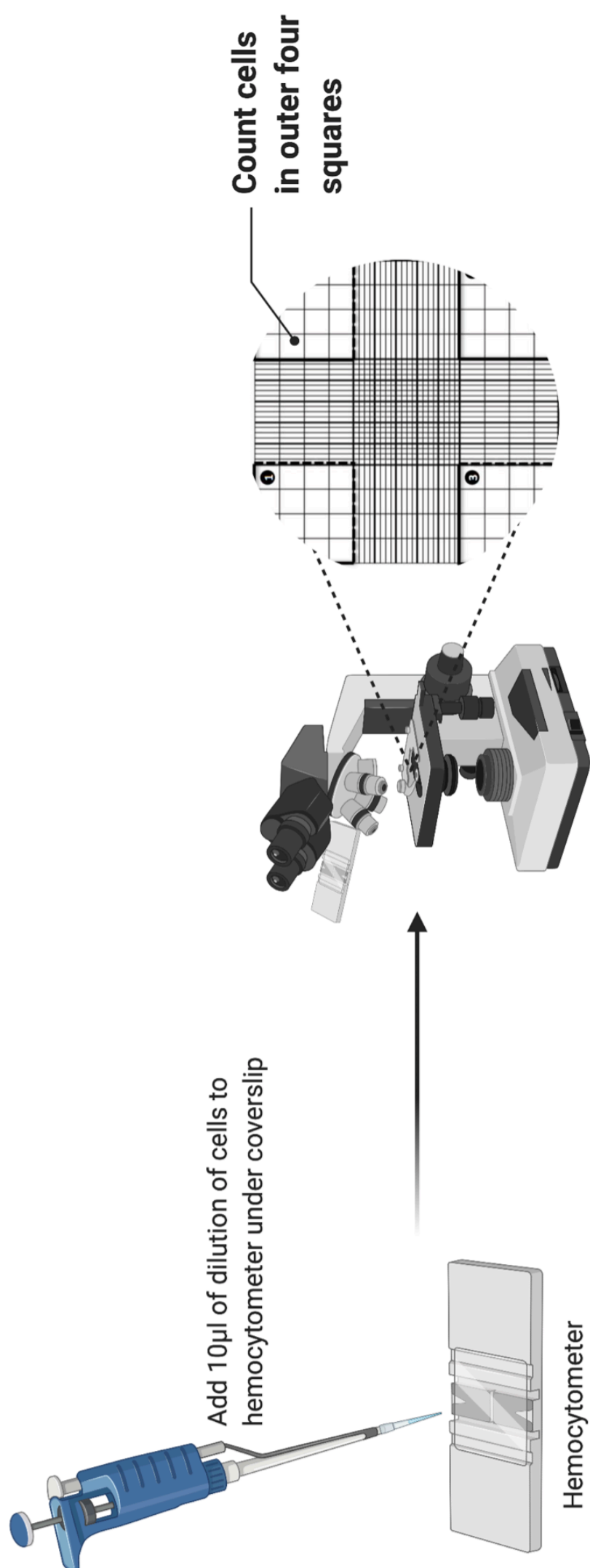
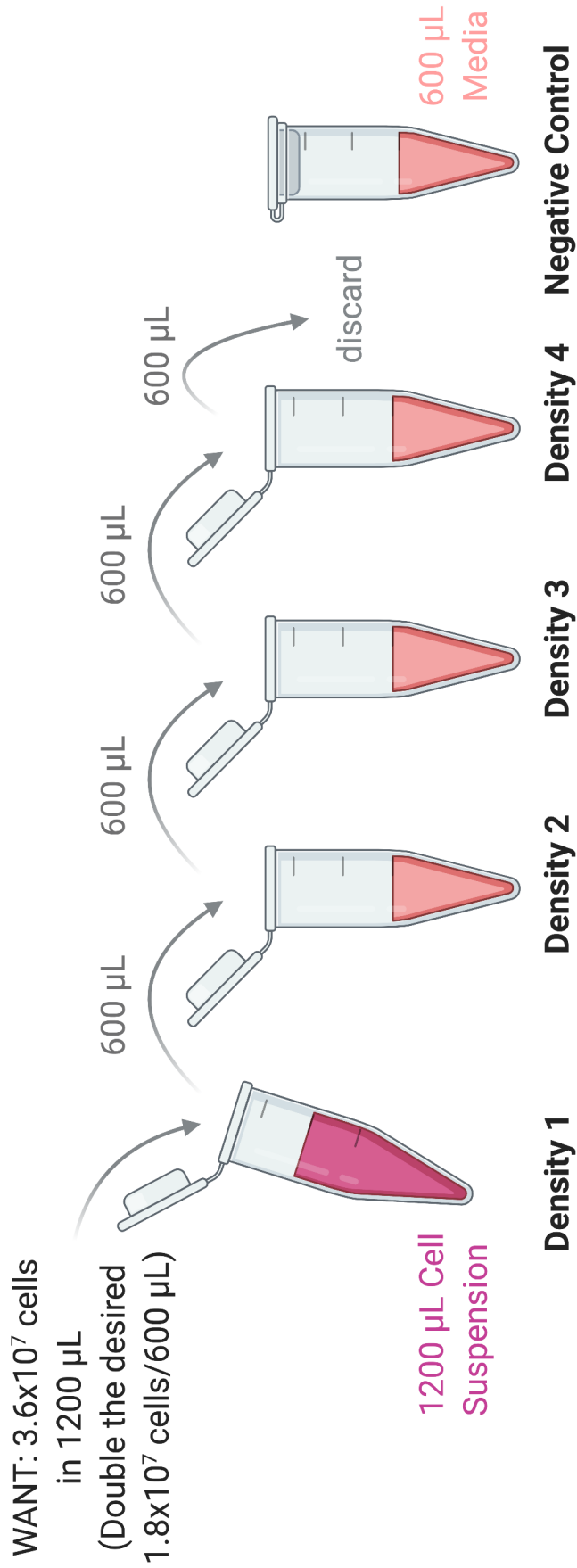


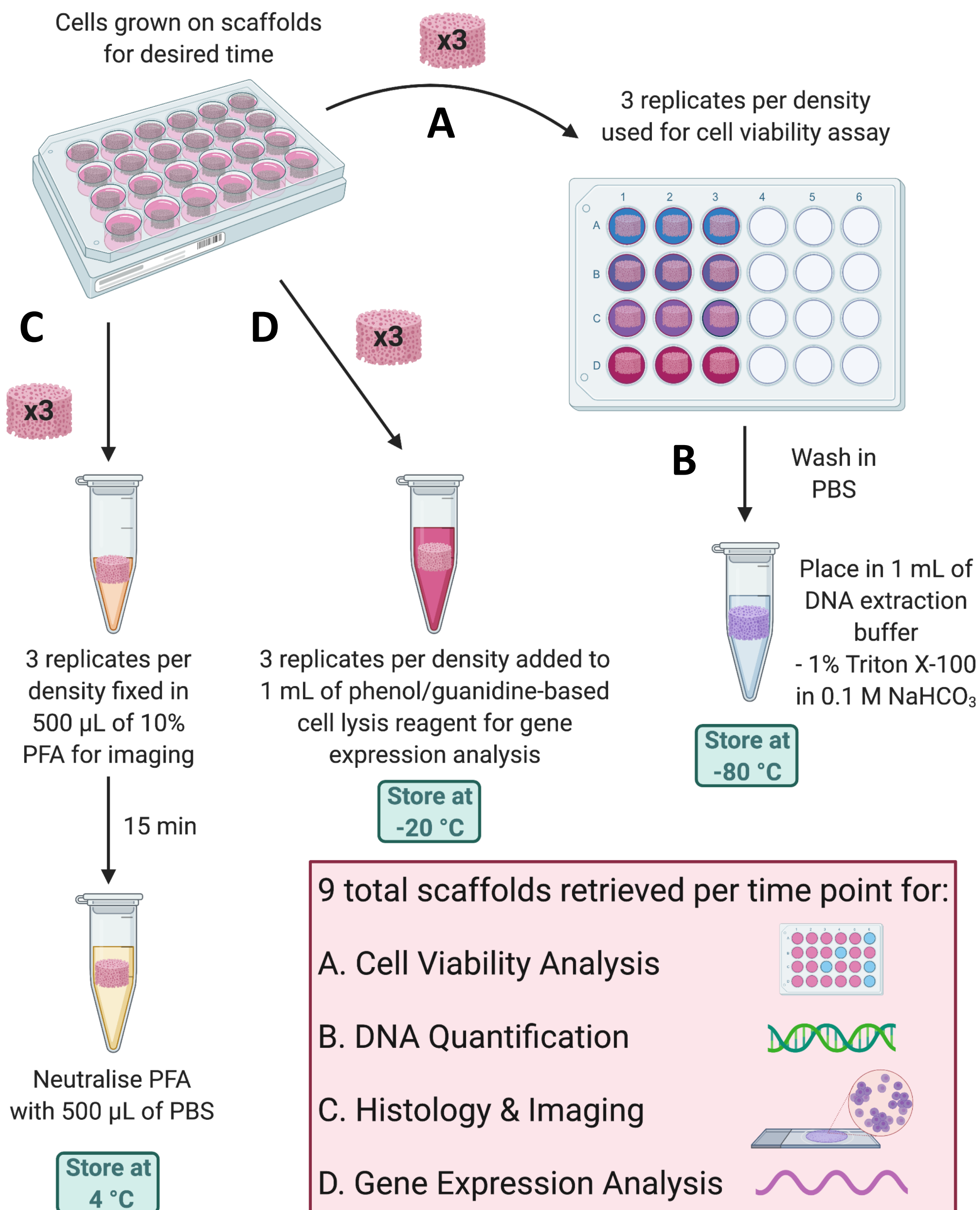
Figure 2

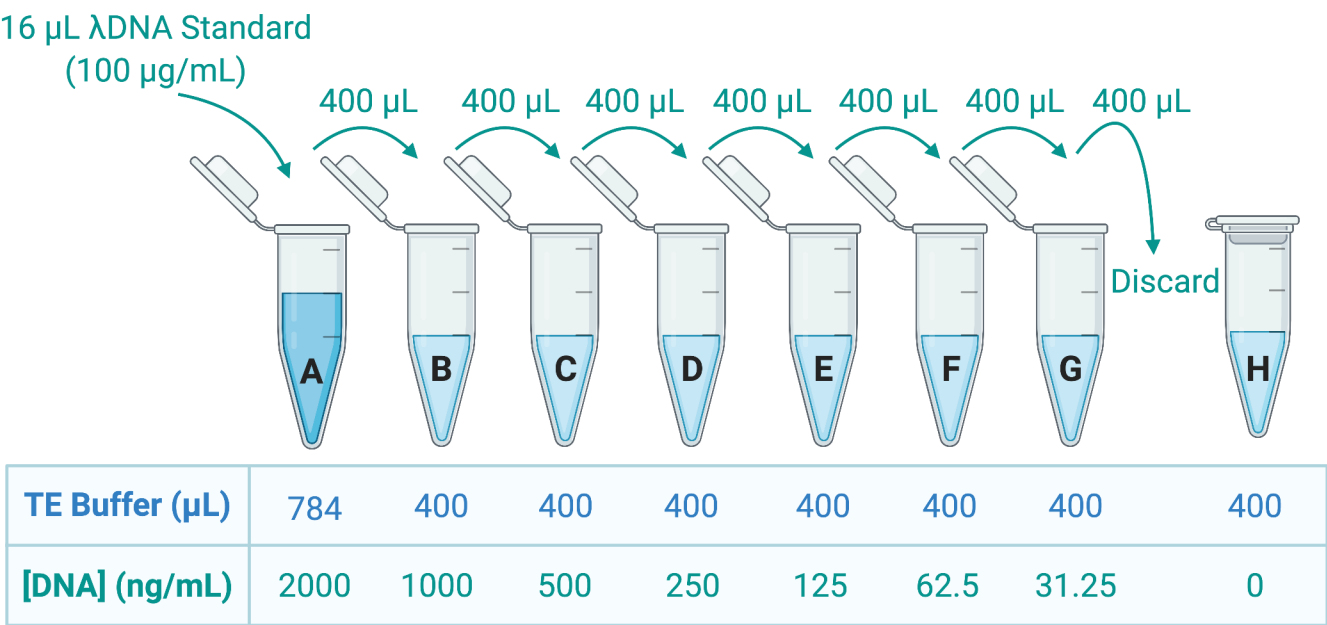




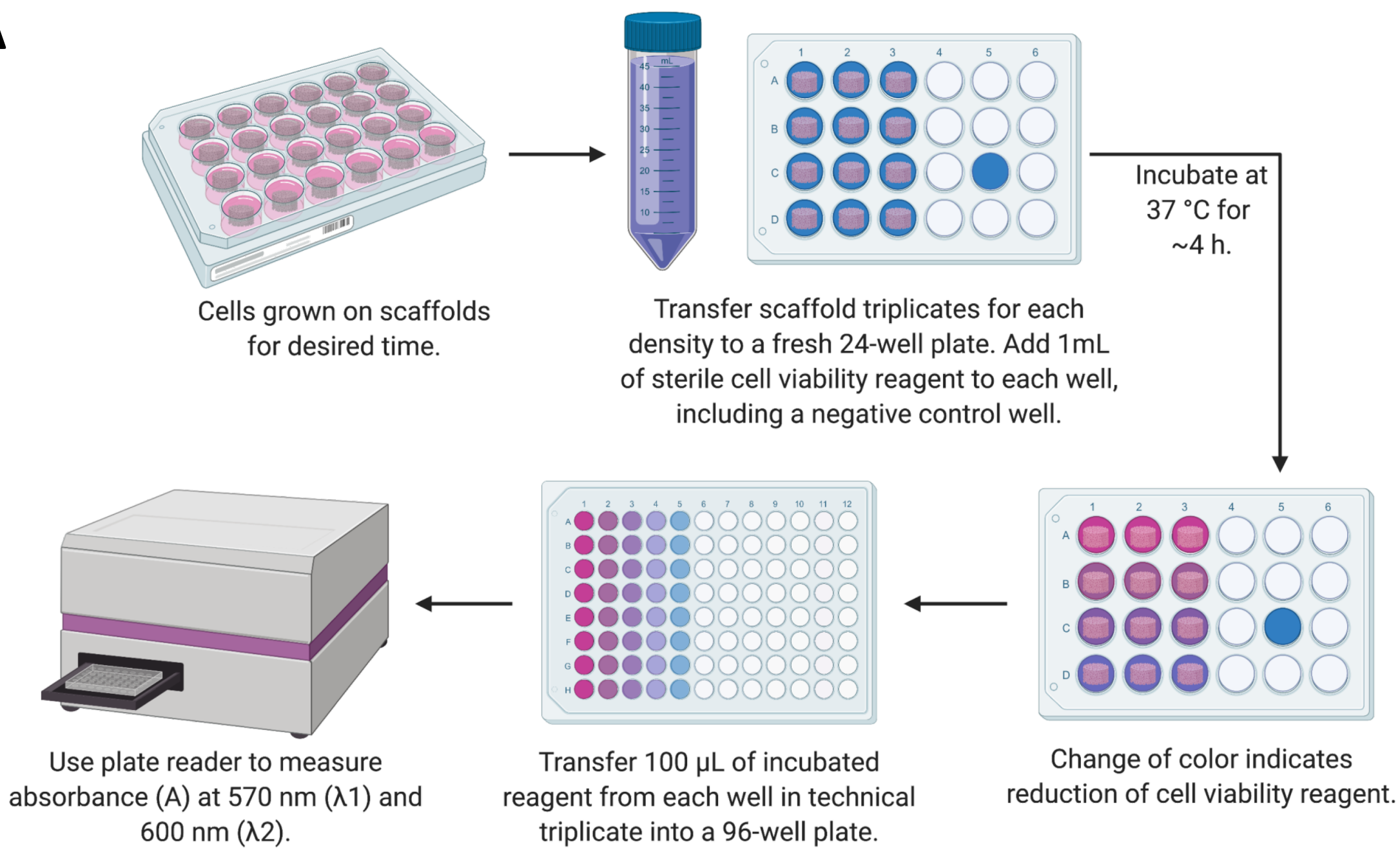


A. Desired cell density per scaffold (20 $\mu\text{L}$ ):	$6 \times 10^5$	$3 \times 10^5$	$1.5 \times 10^5$	$7.5 \times 10^4$	0
B. Cells needed per 30 scaffolds (600 $\mu\text{L}$ ):	$1.8 \times 10^7$	$9 \times 10^6$	$4.5 \times 10^6$	$2.25 \times 10^6$	0

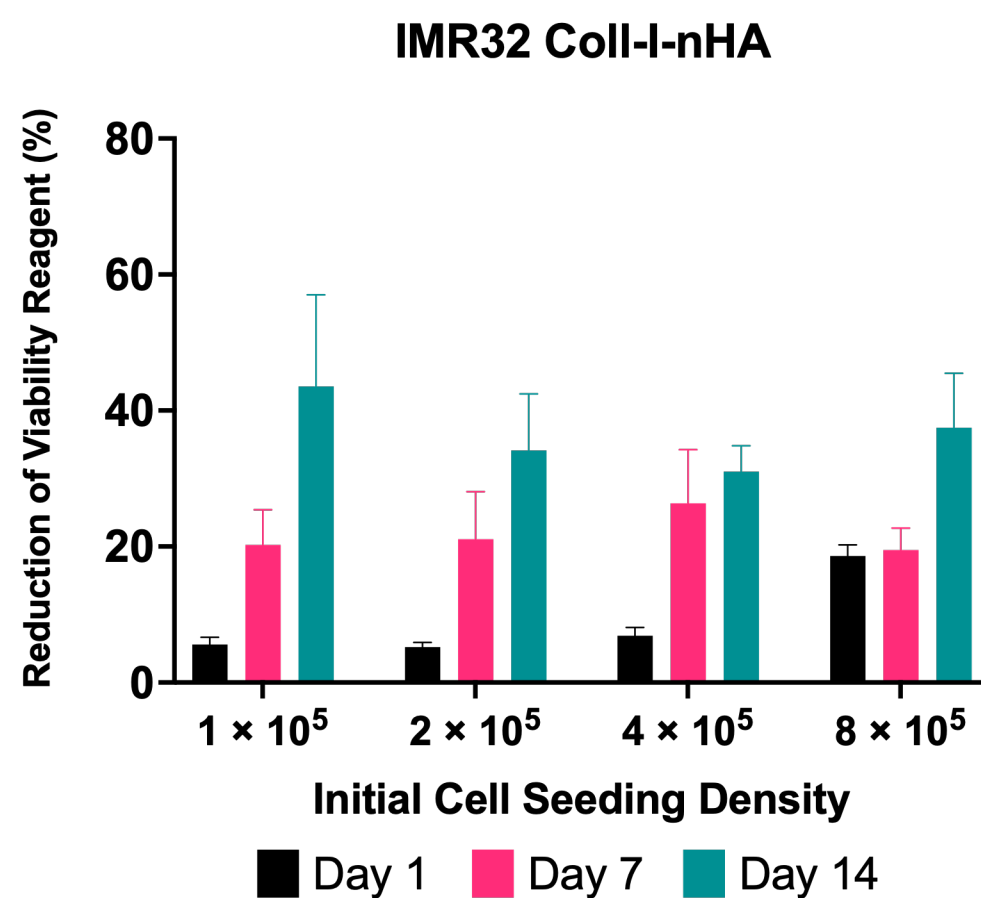
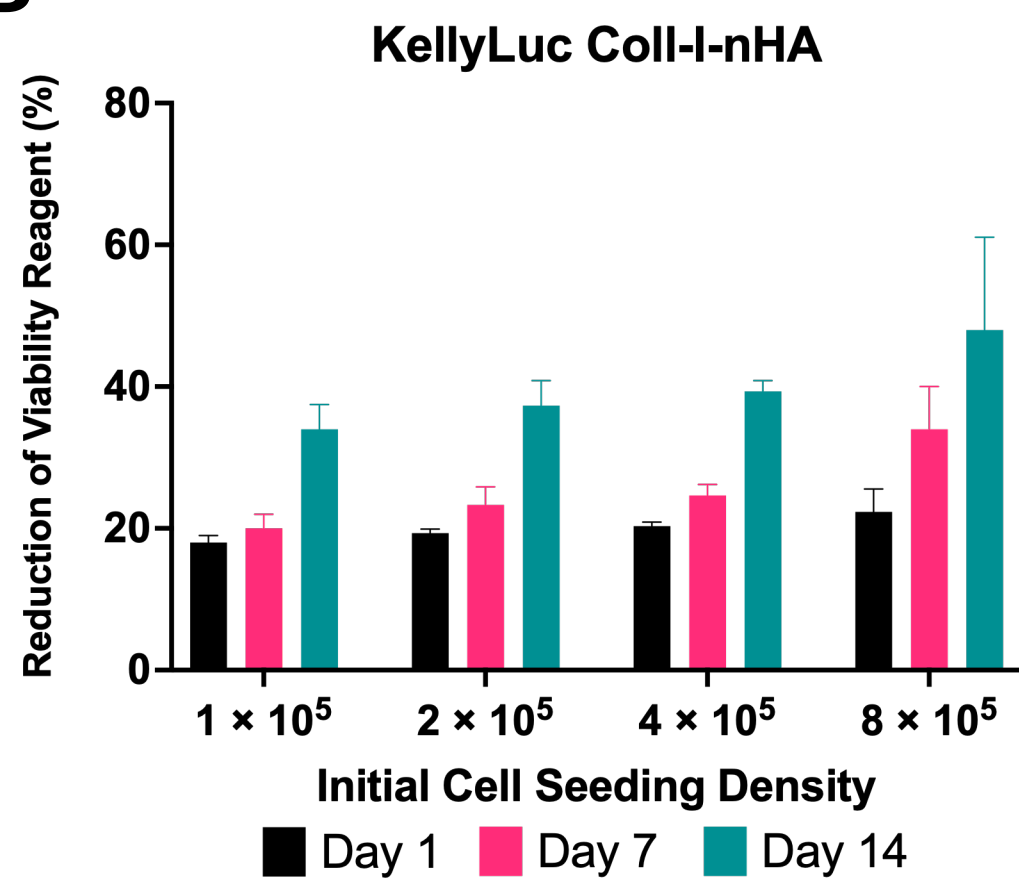




**A**



**B**



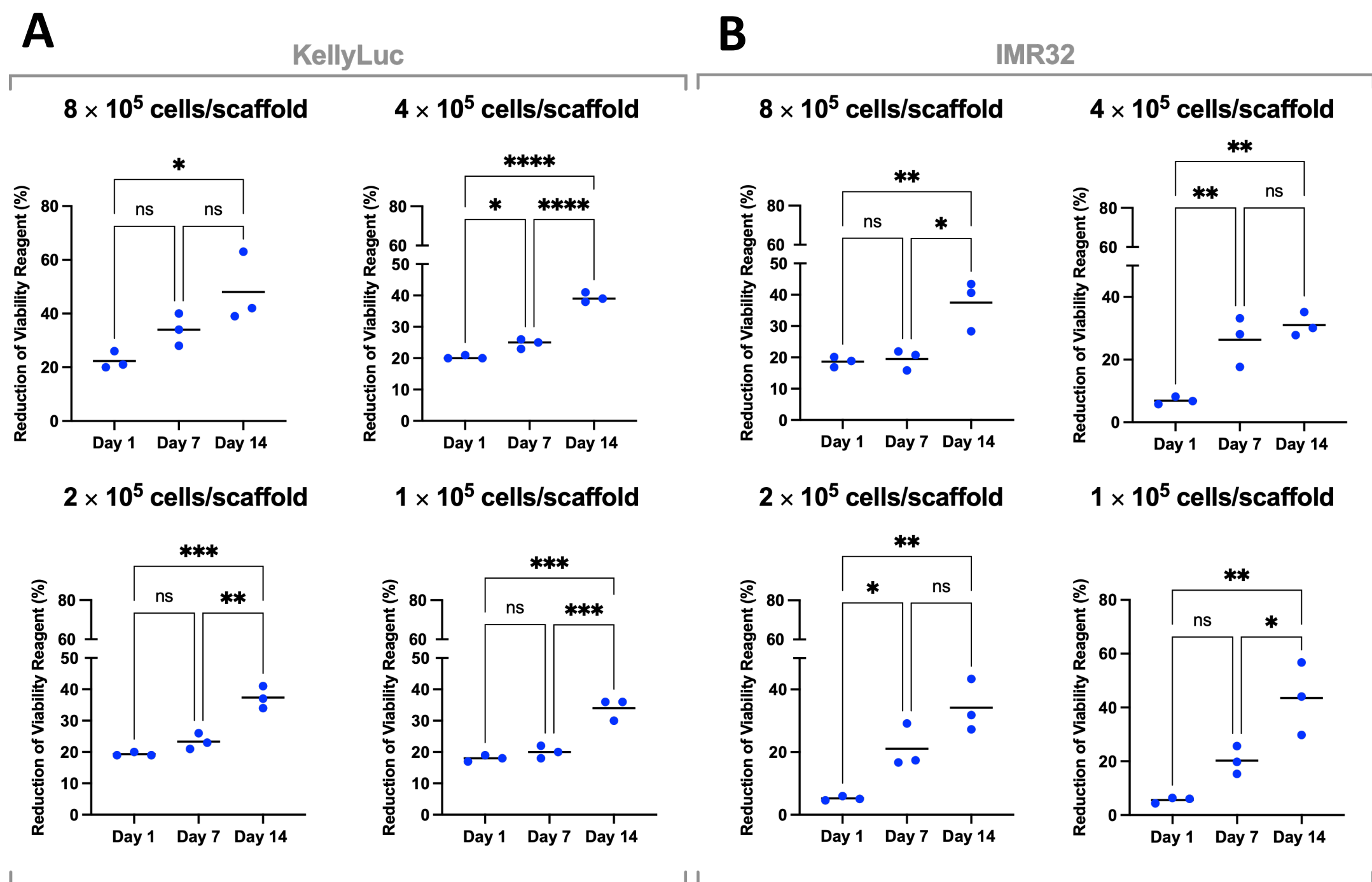
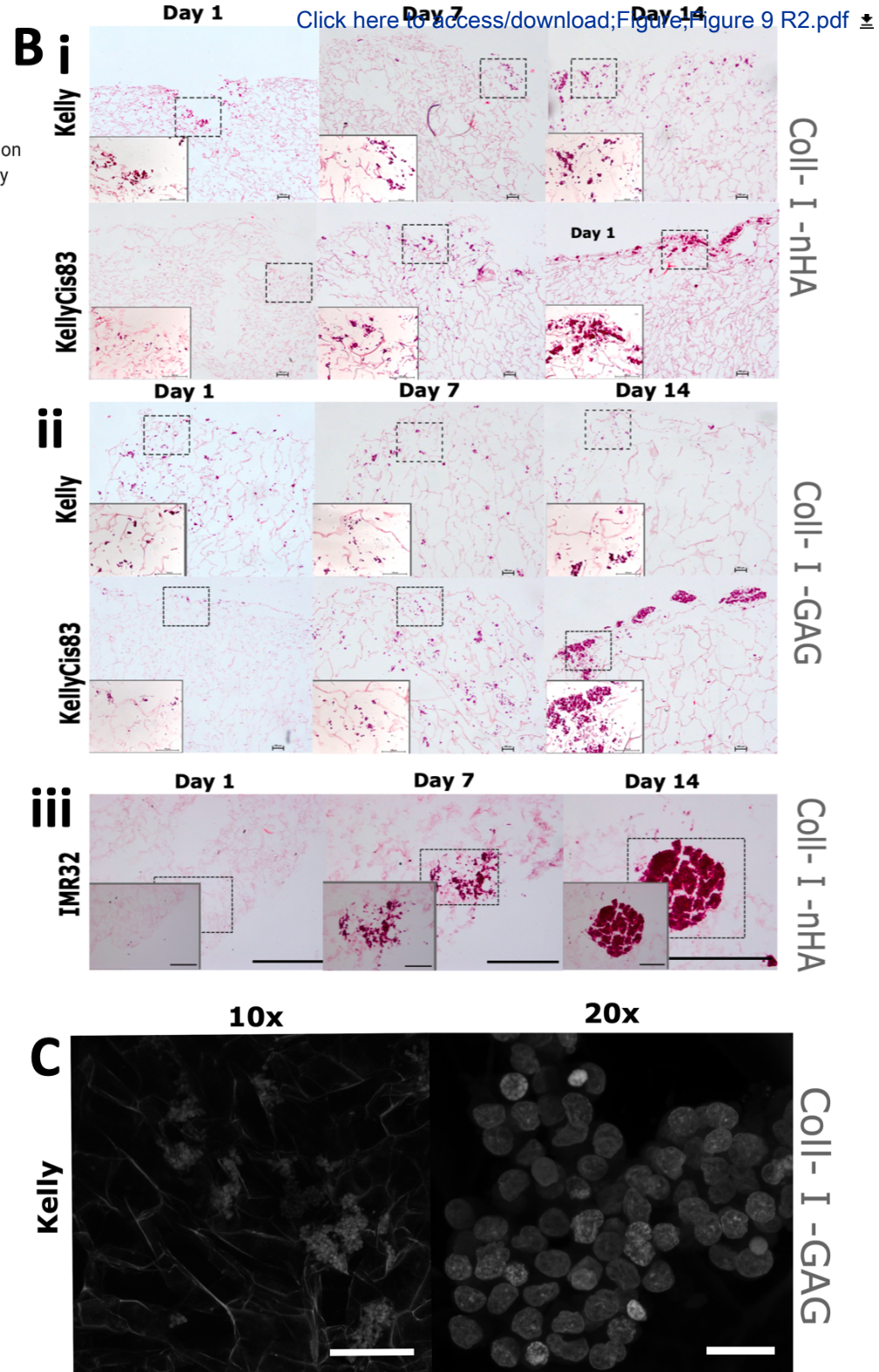
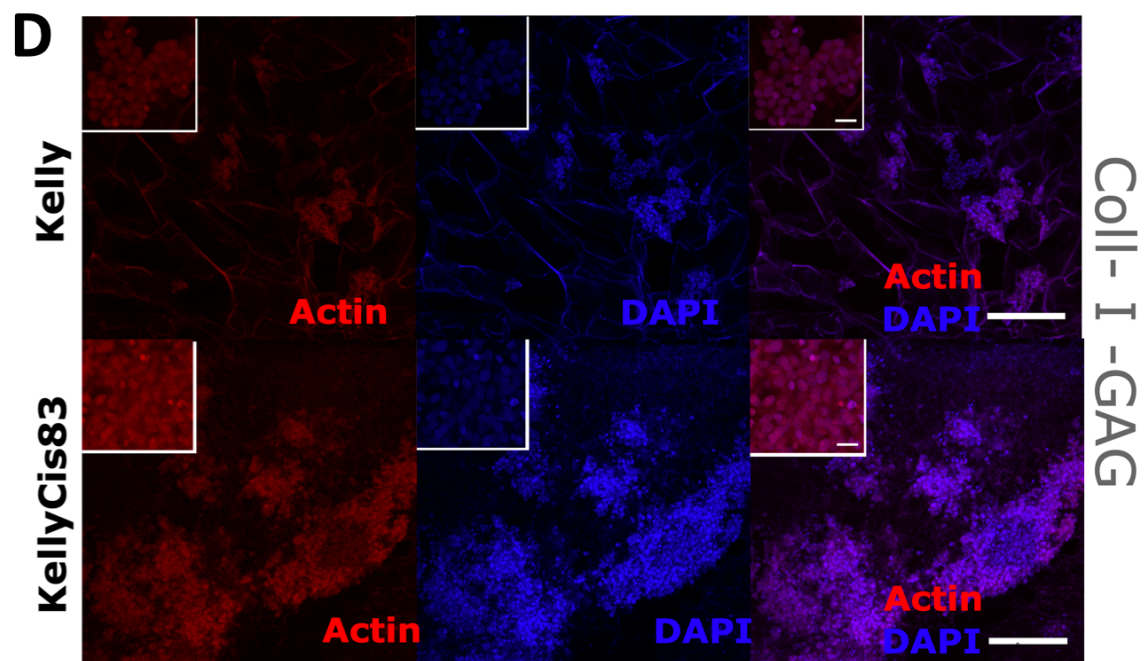
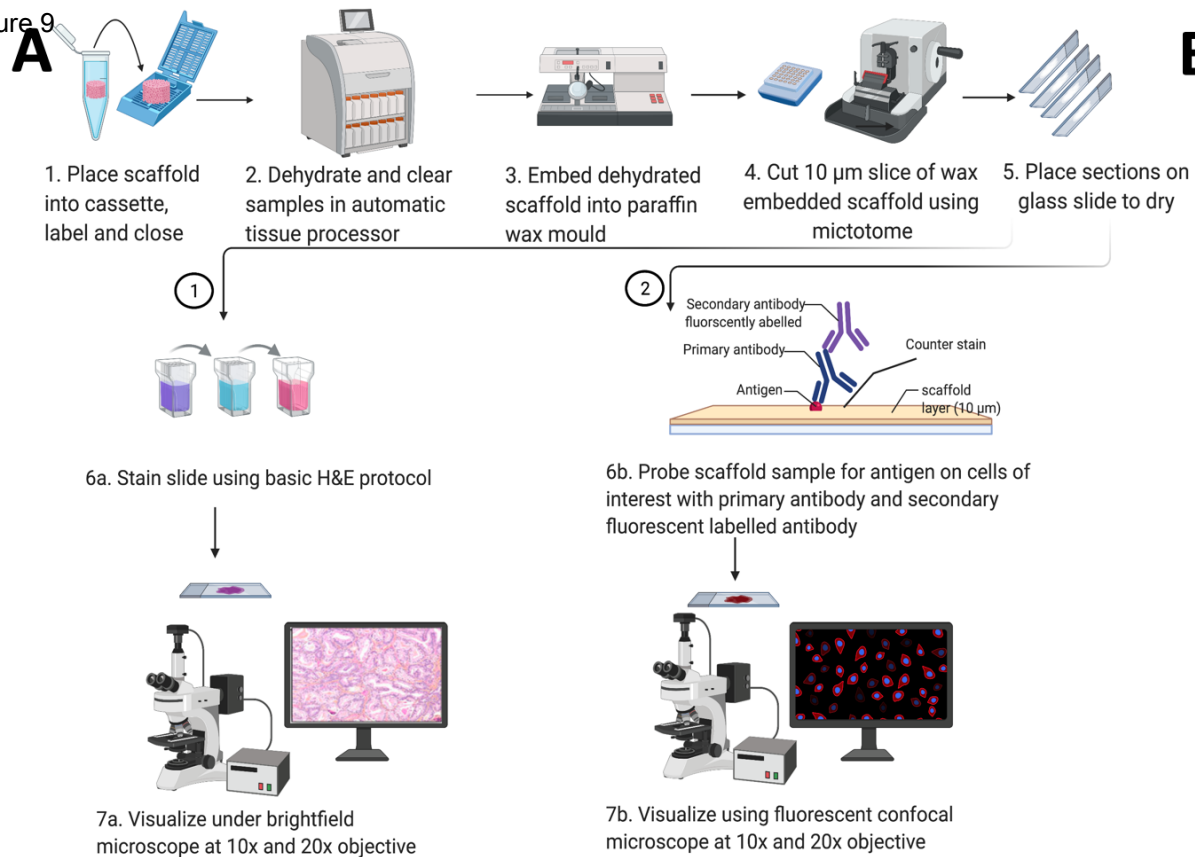


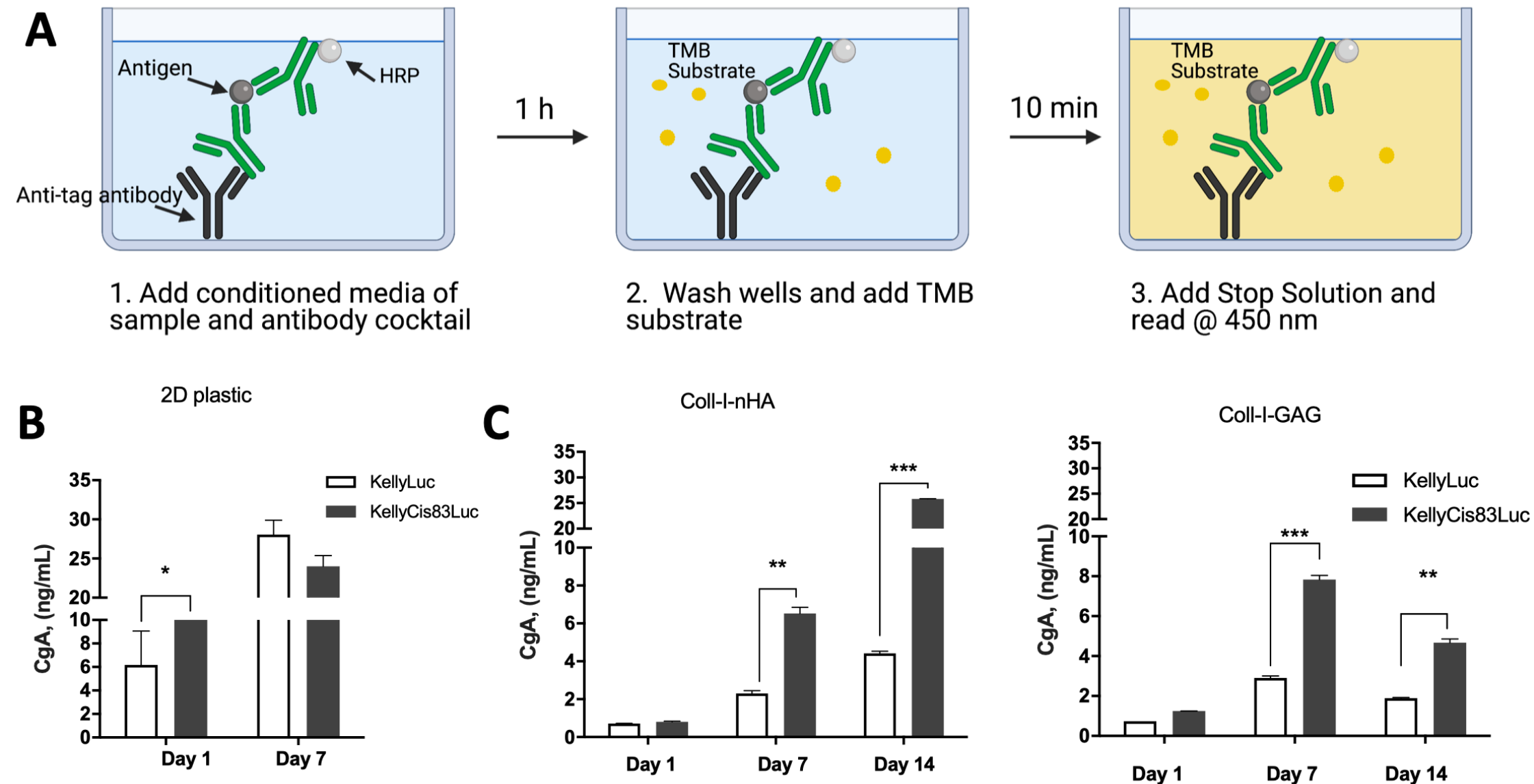




Figure 9









	<i>Coll-I-GAG</i>	<i>Coll-I-nHA</i>
Scaffold Size (diameter [mm] x height [mm])	6 x 4 <sup>17</sup>	6 x 4 <sup>17</sup>
Collagen Concentration (wt. %)	0.5 <sup>17</sup>	0.5 <sup>17</sup>
Substrate Concentration (wt. %) [based off weight of collagen]	0.05 <sup>15,17</sup>	200 <sup>17</sup>
Mean pore size (µm)	96 <sup>22</sup>	96 – 120 <sup>29</sup>
Porosity (%)	99.5 <sup>23</sup>	98.9 – 99.4 <sup>27</sup>
Stiffness (kPa)	1.5 <sup>27</sup>	5.5 - 8.63 <sup>29</sup>

Name of Material/ Equipment	Company	Catalog Number
<b>Cells</b>		
IMR-32	ATCC	CCL-127
Kelly	ECACC	82110411
KellyCis83	Made in lab – deriv -	
SH-SY5Y	ATCC	CRL-2266
<b>Disposable</b>		
0.22 µm syringe filter	Millex	SLHP033RS
1.5 mL Eppendorf tube	Eppendorf	0030 120.086
100 mL sterile Pot	Starstedt	-
10 mL plastic pipette	Cellstar	607 180
15 mL Falcon tube	Starstedt	62.554.502
25 mL plastic pipette	Cellstar	760 180
50 mL Falcon tube	Starstedt	62.547.254
5 mL plastic pipette	Cellstar	606 180
6 mm Biopsy punches	Kai Medical	BP-60F
Aluminium foil	-	-
Cover Slip	Menzel-Glaser	-
HYPERflask	Corning	CLS10030
Microscope slides	Thermo Scientific	J1840AMNT
Opaque black 96-well plate	Costar	3915
Sterile P10 tips	Starlab	S1121-3810
Sterile P1000 tips	Starlab	S1122-1830
Sterile P20 tips	Starlab	S1123-1810
Sterile P200 tips	Starlab	S1120-8810
T-175 (175 cm <sup>2</sup> flask)	Sarstedt	83.3912
T-75 (75 cm <sup>2</sup> flask)	Sarstedt	83.3911.302
Translucent clear 96 well plate	Cellstar	655180
Translucent non-adherent 24 well plates	Cellstar	83.3922.500
<b>Equipment</b>		
Autoclave	Astell	-
Automatic tissue processor	Leica	TP1020
Centrifuge 5804	Eppendorf	-
Hemocytometer	Hausser Scientific	-
Incubator	ThermoScientific	-
Microtome	Leica	RM2255
Oven	Memmert	
P10 pipette	Gilson	
P100 pipette	Gilson	
P1000 pipette	Gilson	
P20 pipette	Gilson	
P200 pipette	Gilson	
Paraffin section flotation bath	Electrothermal	MH8517
Pipette electronic dispenser	Corning	StripipetterUltra
Plate cooler	Leica	EG1140C

Refrigerator -20 °C	Liebherr	-
Refrigerator -80 °C	Liebherr	-
Refrigerator 4 °C	Liebherr	-
Seesaw Rocker	DLAb	SK-D1807-E
Spectrophotometer – Victor <sup>3</sup> V Platereader	PerkinElmer	1420
Tissue culture hood/Laminar flow hood	GMI	8038-30-1044
Tissue Lyser	Qiagen	TissueLyser LT
Tweezers	-	-
Water bath	Grant	-
Wax embedder	Leica	EG1140H

### Materials

1 L Water	Adrona - Bioscienc	568
1% Triton-X	Sigma Aldrich	9002-93-1
10x PBS tablets	Sigma Aldrich	P4417-100TAB
37% paraformaldehyde	Sigma-Aldrich	F8775
Alamar Blue Cell Viability Reagent	Invitrogen	DAL1100
Collagen- glycosaminoglycan scaffold	Tissue engineering research group (TERC	
Collagen-nanohydroxyapatite scaffold	Tissue engineering research group (TERC	
dH <sub>2</sub> O	Adrona - Bioscienc	568

Eosin	Sigma-Aldrich	E4009
-------	---------------	-------

EtOH	Sigma-Aldrich	1.00983.2500
F12	Gibco	21765-029
FBS	Gibco	10270-106
Hemaytoxylin	Sigma-Aldrich	HHS32-1L
L-Glutamine	Gibco	25030-024
MEM	Gibco	21090-022
miRNA easy Kit	Qiagen	217004
MNEAA's	Gibco	11140-035
Penicillin/streptomycin	Gibco	015140-122
Qiazol	Qiagen	79306
Quant-iT PicoGreen dsDNA Assay Kit	Invitrogen	P11496
RPMI	Gibco	21875-034
Sodium bicarbonate	Sigma Aldrich	S7795-500G
Tissue embedding Medium	Sigma	A6330-4LB
Trypsin-EDTA	Gibco	25300-054

### Software

Excel	-	Excel 2016
ImageJ	-	-
Prism	-	Version 9

## Comments/Description

Increasing exposure to cisplatin. Cross resistance acquired

Calibrated by: Cruinn diagnostics Ltd

Calibrated by: Cruinn diagnostics Ltd  
Calibrated by: Cruinn diagnostics Ltd  
Calibrated by: Cruinn diagnostics Ltd  
Calibrated by: Cruinn diagnostics Ltd  
Calibrated by: Cruinn diagnostics Ltd

i)

i)

Made as per: (Cunniffe et al., 2010,  
Fitzgerald et al., 2015; O'Brien et al.,  
2005)

Made as per: (Cunniffe et al., 2010,  
Fitzgerald et al., 2015; O'Brien et al.,  
2005)

10-May-2021

Dear Editor,

In response to review comments for manuscript titled '**A 3D collagen-based scaffold model of the neuroblastoma microenvironment**'. Firstly, we would like to sincerely thank all reviewers for their time and expertise in evaluating our work. We appreciate the comprehensive and constructive appraisal of our manuscript and have addressed their concerns. We believe that our revisions suggested by the reviewers have significantly improved the data presentation and interpretation, and the quality of our manuscript.

We have comprehensively revised our main manuscript text in relation to sentence structure, mistypes, figure mentions and text clarity. To facilitate navigation through the revised manuscript, we used **red text** to track our changes.

### **Reviewer comments**

#### **Editorial request:**

1. Please take this opportunity to thoroughly proofread the manuscript to ensure that there are no spelling or grammar issues.

*Author's response: The authors have proofread the manuscript and are confident that there are no spelling or grammatical issues.*

2. Please revise the following lines to avoid previously published work: 85-86, 92-97, 100-102.

*Author's response: The authors have restructured the sentences from these lines to avoid previously published work and have referenced previous work appropriately.*

3. Please revise the text to avoid the use of any personal pronouns (e.g., "we", "you", "our" etc.).

*Author's response: The authors have ensured there is no use of personal pronouns in the methodology section of the manuscript. However, we feel it is appropriate to keep some personal pronouns in the discussion section (e.g., "Here we described", "We aimed", etc.)*

4. JoVE cannot publish manuscripts containing commercial language. Please remove all commercial language from your manuscript and use generic terms instead. All commercial products should be sufficiently referenced in the Table of Materials: e.g., HYPERflask, Corning, Falcon, Eppendorf, Alamar Blue, PicoGreen, QIAzol, miRNeasy, etc. We must maintain our scientific integrity and prevent the subsequent video from becoming a commercial advertisement.

*Author's response: The authors have removed commercial language from the manuscript, substituting with appropriate generic terms, as below:*

*HYPERflask – Multilayer cell culture flask (or multilayer flask)*

*Falcon/Eppendorf - Centrifuge tube*

*Alamar Blue – Cell viability assay (reagent)*

*PicoGreen – Fluorescent double-stranded (ds)DNA stain*

*QIAzol - Phenol/guanidine-based cell lysis reagent*

*MiRNeasy - an appropriate RNA extraction kit*

5. Please adjust the numbering of the Protocol to follow the JoVE Instructions for Authors. For example, 1 should be followed by 1.1 and then 1.1.1 and 1.1.2 if necessary. Please refrain from using bullets or dashes.

*Author's response: The authors have adjusted numbering and have not used letters/bullets/dashes.*

6. Please ensure that all text in the protocol section is written in the imperative tense as if telling

someone how to do the technique (e.g., “Do this,” “Ensure that,” etc.). The actions should be described in the imperative tense in complete sentences wherever possible. Avoid usage of phrases such as “could be,” “should be,” and “would be” throughout the Protocol. Any text that cannot be written in the imperative tense may be added as a “Note.” However, notes should be concise and used sparingly. Please include all safety procedures and use of hoods, etc.

*Author's response: The authors have ensured the protocol section is written in the imperative tense.*

7. Line 149-151: Please ensure that the Protocol section consists of numbered steps. We cannot have non-numbered paragraphs/steps/headings/subheadings.

*Author's response: The authors have ensured that protocol sections consist of numbered steps with short “Notes” at the top of the subsection if additional information is required.*

8. Please include a one-line space between each protocol step and then highlight up to 3 pages of the Protocol (including headings and spacing) that identifies the essential steps of the protocol for the video, i.e., the steps that should be visualized to tell the most cohesive story of the Protocol. Remember that non-highlighted Protocol steps will remain in the manuscript, and therefore will still be available to the reader.

*Author's response: A one-line space has been added between each step in the protocol and 3 pages have been highlighted for the video: from section 4.3 to 5.1 inclusive.*

9. Please include the limitations of the protocol and the troubleshooting techniques in the discussion section.

*Author's response: A discussion of the protocol limitations has been added to the discussion at page 22, lines 916-931.*

10. Please obtain explicit copyright permission to reuse any figures from a previous publication. Explicit permission can be expressed in the form of a letter from the editor or a link to the editorial policy that allows re-prints. Please upload this information as a .doc or .docx file to your Editorial Manager account. The Figure must be cited appropriately in the Figure Legend, i.e. “This figure has been modified from [citation].”

*Author's response: Copyright permission has been requested to reuse some components of Figure 10 from previously published work by Curtin C. et al, 2018.*

*This permission will be uploaded to the Editorial Manager account once we receive it. Meanwhile, we uploaded the link to the editorial policy. The figure has been appropriately cited in the manuscript, page 21 line 872 “This figure has been adapted from Curtin et al., 2018<sup>17</sup>, an open access article under the CC BY-NC-ND license 4.0.”*

11. For in-text formatting, corresponding reference numbers should appear as numbered superscripts after the appropriate statement(s).

*Author's response: In-text citations have been modified to appear as numbered superscripts.*

12. Please do not use the &-sign or the word “and” when listing authors. Authors should be listed as last name author 1, initials author 1, last name author 2, initials author 2, etc. End the list of authors with a period. Example: Bedford, C. D., Harris, R. N., Howd, R. A., Goff, D. A., Koolpe, G. A. Quaternary salts of 2-[(hydroxyimino)methyl]imidazole. Journal of Medicinal Chemistry. 32 (2), 493-503 (1998).

*Author's response: The bibliography has been modified to meet these requests.*

13. Figure 5/ 6/7: Please replace the commercial terms (Alamar Blue, QIAzol, etc.) by generic terms.

*Author's response: Commercial terms have been removed from figures and figure legends.*

14. Figure 8: Please replace the commercial terms (PicoGreen, etc.) by generic terms.

*Author's response: Commercial terms have been removed from figures and figure legends.*

15. Figure 9: Please include scale bars for all the images in the panel (eg., B iii)

*Author's response: Appropriate scale bars have been added to Figure 9. Legend corresponding to figure 9 has been adjusted to inform reader of the appropriate scaling of images, page 20 line 836-850..*

16. Figure 10: Please revise the Y axis legend to include the units within parenthesis.

*Author's response: Units on the Y axis have been included within parenthesis (ng/ml).*

17. Please maintain a single space between the numeral and (abbreviated) unit, except in cases of %, x, and ° (i.e., the degree sign; excluding temperature) in the Table of Materials. Examples: 5 mL, 10%, 3°, 100 °C, 3x, SSC

*Author's response: Spaces have been used before units as requested, with the exception of %, x, and °.*

## **Reviewer 1**

Summary: in the article "A 3D collagen-based scaffold model of the neuroblastoma microenvironment" the authors described a number of standard lab methodologies that can be applied for the analysis of 3D scaffolding model of neuroblastoma. Although the title of their work is very interesting and inviting for reading, the methodologies described are lowering the value of the title.

### Major Concerns:

The title of the manuscript needs to be adopted to its context. What one would expect is to see how the authors produced, managed and analysed the 3D scaffolding system and its microenvironment created after 14 days of neuroblastoma cell growth while comparing it with the native metastatic neuroblastoma milieu. Instead, the focus of the work is viability and morphological assessments of cell lines grown in 3D conditions.

*Author's response: The authors have taken this into consideration and re-titled our manuscript, 3D in vitro biomimetic model of neuroblastoma using collagen-based scaffolds. This is a methodology paper that demonstrates how some already extensively characterised 3D bio-engineered platforms can be adopted or repurposed to study a different tissue pathology in a minimal format. We believe that it is sufficient to incorporate a more detailed collagen-based scaffolds features and manufacturing in order to describe this acellular component of the proposed 3D in vitro platform (Haugh et al., 2010; Fergal J. O'Brien et al., 2004) and focus more on characterisation of the cellular component as this is essential to study neuroblastoma biology and/or carry out drug screening. A table with the physical properties of the two scaffolds has been added to the text at page 4, line 133. Additional manufacturing information has been added also to the introduction section page 3 line 116-131. Both scaffolds are manufactured with identical blending, freeze-drying, sterilisation and crosslinking protocols.*

### Minor Concerns:

The reviewer is wondering why the scaffolds are kept first in adherent and only after 24h moved to low-adhesion plates? In order to allow that all the cells attach to the scaffold, wouldn't it be better to place them immediately in these types of plates?

*Author's response: We appreciate this comment. This was our oversight. The authors can confirm non-adherent plates are used throughout the whole experiment. They are used immediately when plating cells at Day 0 and scaffolds are transferred to new non-adherent plates at Day 1. This has been addressed in the text, page 10 line 402 and page 11 line 432 - 436, to better clarify to the reader they are used for the entirety of the experiment.*



## Reviewer 2

### Minor Concerns:

Two different scaffold compositions are considered, but in the protocol, it isn't considered the physical characterization of scaffolds as porosity, young modulus, or swelling. Would be interesting for other scientists to include a section of scaffolds characterisation

*Author's response: We appreciate this comment. The proposed 3D model has acellular and cellular components. Since the focus is on the cellular component, the paper would benefit additional information regarding acellular component. A table with the physical properties of the two scaffolds has been added to the text at page 4, line 133. Additional manufacturing information has been added also to the introduction section page 3 line 109-131. Both scaffolds are manufactured with identical blending, freeze-drying, sterilisation and crosslinking protocols. Making scaffolds reproducible. Scaffolds only differ in the bio-composite additions to the scaffolds.*

## Reviewer 3

Summary: The manuscript by Gallagher et al aims to reverse engineer the neuroblastoma microenvironment using 3D collagen scaffolds functionalized with nHA and GAG. The manuscript is well written and provides sufficient step-by-step protocols which can be easily followed.

The scaffold has a dimension of 6 mm in diameter and 4 mm in thickness. This reviewer is wondering about the nutrient or drug diffusion into the scaffolds. Would the authors briefly comment on this?

*Author's response: We would thank the reviewers for this consideration. We are confident that the collagen-based scaffolds used in this protocol have been optimised in depth to create manufacturing methods that create homogenous pore sizes and structure, conducive to allow cells to grow, infiltrate and allow nutrient and drug diffusion (Haugh et al., 2010; Fergal J. O'Brien et al., 2004). However, we have briefly commented on potential uneven nutrient distributions within the scaffolds on page 22, line 917-920. Curtin et al., 2018 describes both the Coll-I-GAG and Coll-I-nHA scaffolds required drug concentrations that matched clinically relevant values of that seen in vivo to mount a response on NB cell lines in 3D environment. The dose response of Kelly and KellyCis83 NB cell lines was 8-14 and 80-140 times higher, respectively, in the cell's grown in 3D scaffolds compared to 2D. Although the exact diffusion rates into scaffold are unknown, with this previously published data we can trust that the diffusion rates are to a higher physiologically relevant degree than 2D in vitro models.*

In general, Alamar blue assay could be used to determine cell numbers. In my opinion, it would be more appropriate to perform a standard curve (cell number vs fluorescence signal) and calculate the fluorescence signal result back into „cell number“, rather than % reduction. The author also mentioned on page 18 line 743-746 that the Alamar Blue assay to be a simple and effective technique to support DNA quantification data. Do results (calculated cell number) from Alamar blue assay correlate to PicoGreen assay (Figure 7 vs 8)?

*Author's response: We appreciate this comment, however we feel a standard curve is slightly more difficult given the 3D nature of this model. To generate a standard curve 2D plated cells would need to be used, and so the fluorescent signal may not be comparative to cells growing within 3D scaffolds. Adding to this, there is a possibility that some cells will have a higher metabolic rate than others, and so it is difficult to accurately convert to viable cell numbers. Therefore, we opted to look at the percentage reduction of the Alamar Blue reagent by cells, including a blank which contained Alamar Blue reagent diluted in full growth media, lacking only the cells in scaffolds. In the results on page 17, we have added a section comparing the results from Alamar Blue and PicoGreen assays from lines 711-*

715. There were some differences in the growth trends for specific samples, however overall, the trends obtained from the two assays were consistent, and we feel that inclusion of both assays increases our confidence when examining these trends. Importantly, in many experimental strategies scientists look at relative changes rather than absolute, e.g. how metabolism on day 7 is different to day 1 or how cell viability changed in response to a drug? So, it is essential to run 2-3 different but robust assays to evaluate cell behaviour, gather data and accurately interpret the results.

Please also discuss that fluorescence interference from test compounds can be influenced the analysis of the Alamar Blue assay

*Author's response: The authors have taken this point into consideration. They feel the appropriate controls are in place to account for inference from test compounds that may be influencing the cell viability assay. A brief overview of experimental design of the cell viability assay to account for inference; The cell viability assay was carried out under the same experimental protocols for each day of analysis. Flat bottom plates were used for each cell viability assay, as it is known that differing round and flat bottom plates can interfere with the cell viability assay reading. The blank used for the assay was the media that the cells were grown in, this eliminated interference from serums (e.g. FBS) (Goegan et al., 1995; Page et al., 1993).*

The authors mentioned on Page 18 line 755 that the 3D models enable cell growth and infiltration visualization. Cell growth can be addressed using qualitative biochemical assays. This reviewer is wondering if the cell infiltration can be qualitatively analysed in this 4mm-thick scaffold

*Author's response: Traditionally, to assess infiltration into scaffolds, scaffolds are fixed and undergo tissue processing. They can then be embedded in paraffin wax and cut into thin sections for histological staining and imaging. If the scaffold is embedded in a sideways orientation, it is possible to stain and image whole scaffolds from the side-view, enabling visualisation and qualitative assessment of cell infiltration and distribution throughout the scaffolds. Image data can then be converted to a % infiltration for quantitative assessment. We describe the preparation of scaffolds for histological staining in section 5.3, lines 568-658, and sample images of scaffold sections stained with H&E can be seen in Figure 9.*

This reviewer would suggest some recent works that can be considered to add to the introduction (if the author feel that it actually adding value to their manuscript):

1. A general review of ECM characteristics and reverse-engineering of the tumor microenvironment can be considered to add in the introduction: Ouellette JN et al 2021 Bioengineering; Sapudom J et al 2018 Biomaterials Science.

2 On Page 3 line 94-97. The collagen-hydroxyapatite scaffold has also been used as a cell culture model of the tumor microenvironment (He F et al 2019 Biomaterials).

3. The author discussed GAG in the ECM. As short discussion of HA on cell behavior would be helpful. For example: It has been known that GAG exhibits molecular specific effects on cell behaviors (Kreger ST et al 2009 Matrix Biology, Sapudom J et al 2017 Acta Biomaterialia, Sapudom J et al 2020 Biomaterials Science).

4. A recent review on potential use of 3D models for drug screening can be considered to add in the introduction (Brancato V et al 2020 Biomaterials).

*Author's response: Thank you for recommending these recent publications. We have assessed all of them, except for "He F et al 2019 Biomaterials" as we could not identify this paper.*

*In lines 75-78 when discussing the importance of the ECM in Cancer, we have added text referencing Brancato 2020 and Ouellette 2021 and their sources.*

*In lines 85-89 when discussing collagen in the ECM we have added text referencing Ouellette 2021.*

*In lines 90-93 when discussing the value of 3D matrices in assessment of cell response to chemotherapeutics we have added text referencing Sapudom 2018.*

*In lines 93-96 when discussing the correlation between 3D models and in vivo studies we have added text referencing Ridky 2010 (from Brancato 2020).*

*Some of the recommended texts focussed specifically on Collagen scaffolds supplemented with hyaluronan (Kreger 2009, Sapudom 2017, Sapudom 2020). In our manuscript, we mention supplementing collagen scaffolds with glycosaminoglycans (GAGs). While hyaluronan/hyaluronic acid is a category of GAG commonly used in scaffolds, we focus on the use of chondroitin-6-sulphate, another category of GAG. We have clarified this in lines 102-103, 112-115 and 118-119. We have maintained use of the abbreviation "Coll-I-GAG" throughout the document for ease of reading and as it has been used in this context in several previous publications referenced in the manuscript (O'Brien 2004, O'Brien 2005, Haugh 2011, Murphy 2010, Haugh 2009). We have not included the references on hyaluronan as it is not within the focus of this paper.*

#### **Reviewer 4**

Summary: In this research, authors in detail described the protocol about studying neuroblastoma microenvironment using 3D collagen-based scaffolds. The manuscript is well presented and the optimizations of the method, particularly the dilution of cell, are very rigorous and detailed.

#### Minor Concerns:

Line 398 and 386, authors should pay attention to unit format.

*Author's response: The authors have corrected all unit formatting throughout the text.*

The difference between Coll-GAG and Coll-nHA, especially mechanical properties, should be discussed.

*Author's response: Thank you for this consideration and we agree that additional information in the introduction on the background of the scaffolds should be given to the reader. A table with the physical properties of the two scaffolds has been added to the text at page 4, line 133. Additional manufacturing information has been added also to the introduction section page 3 line 109-131. Both scaffolds are manufactured with identical blending, freeze-drying, sterilisation and crosslinking protocols. Making scaffolds reproducible. Scaffolds only differ in the bio-composite additions to the scaffolds.*

More explicit explanation of the statistical methods in manuscript is needed.

*Author's response: The statistical methods used to analyse cell viability and DNA quantification results have been added as steps at the end of their respective sections (lines 501-509 and 554-561).*

Once again, thank you all for taking the time to read and analyse the paper submitted. We hope all minor and major concerns have been addressed and look forward to your response.

Your sincerely,

Olga Piskareva  
Corresponding author



10-May-2021

RE: Copyright permission to reuse any figures from a previous publication

Dear Editors,

In the manuscript submitted to JoVE, Figure 10 uses a portion of Figure 3 (A, D and E) published previously by I and co-authors in *Acta Biomaterialia* (Elsevier) as an open access article under the CC BY-NC-ND license 4.0. (<http://creativecommons.org/licenses/by-nc-nd/4.0/>). The full details are as follows: Curtin C, Nolan JC, Conlon R, et al. A physiologically relevant 3D collagen-based scaffold–neuroblastoma cell system exhibits chemosensitivity similar to orthotopic xenograft models. *Acta Biomater.* 2018;70:84-97. doi:10.1016/j.actbio.2018.02.004

While I have requested the permission and expect to get it soon, the details of the license use can be verified at <https://www.elsevier.com/about/policies/open-access-licenses>.

The use of the original Figure 3A, D and E has been appropriately cited in the manuscript, page 21 line 872 “This figure has been adapted from Curtin et al., 2018<sup>17</sup>, an open access article under the CC BY-NC-ND license 4.0.”



About Elsevier Products & Solutions Services Shop & Discover

Once selected, Creative Commons user licenses are non-revocable. We recommend authors check if their funding body requires a specific license. See the [Creative Commons](#) website for more details about what to consider before choosing a user license. [Click here](#) for a full list of user licenses used by Elsevier.

User license	Read, print and download	Redistribute or republish the article (e.g. display in a repository)	Translate the article	Download for text and data mining purposes	Reuse portions or extracts from the article in other works	Sell or re-use for commercial purposes
CC BY 4.0	Yes	Yes	Yes	Yes	Yes	Yes
CC BY-NC-ND 4.0	Yes	Yes	Yes For private use only and not for distribution	Yes	Yes	No
Elsevier user license	Yes	No	Yes	Yes	No	No

Please note: Under the CC BY-NC-ND license and for the Elsevier user license permitted 3rd party reuse is only applicable for non-commercial purposes. For further details on the rights granted to Elsevier see our [copyright information](#) or to obtain permission for commercial use see our [permission information](#). Also note further permission may be required from the rights owner for any content within an article that is identified as belonging to a third party.

Please let me know if any further information is required regarding this issue.

Sincerely yours,



Olga Piskareva,  
Corresponding author  
StAR Research Lecturer  
Department of Anatomy and Regenerative Medicine  
RCSI University of Medicine and Health Sciences  
Dublin Ireland  
E: [olgapiskareva@rcsi.com](mailto:olgapiskareva@rcsi.com)